COMPOSITION AND SOURCE OF THE HYDROTHERMAL FLUIDS OF THE SANTO NIÑO VEIN, FRESNILLO, MEXICO, AS DETERMINED FROM $^{87}Sr/^{86}Sr$, STABLE ISOTOPE, AND GAS ANALYSES

By
Laurie D. Benton

Submitted to the Faculty in partial fulfillment
of the requirements for the degree of
Master of Science

New Mexico Institute of Mining and Technology
Socorro, New Mexico
April 1991

ABSTRACT

The epithermal, Ag-Pb-Zn, Santo Niño vein has been a significant source of ore for the Fresnillo mine since its discovery in 1975. The vein has been the subject of several detailed studies, but the genesis of the vein remains unclear. The objective of this study is to examine two questions regarding the vein's genesis: where the components of the mineralizing fluids originate; and how they change with time? These questions were addressed using $^{87}Sr/^{86}Sr$, stable isotopes, and gas analyses.

Vein calcite $^{87}Sr/^{86}Sr$ compositions are 0.7060 to 0.7091 and quartz-hosted fluid-inclusion solute has corrected $^{87}Sr/^{86}Sr$ values of 0.7064 to 0.7078 with one exception which has a corrected value of 0.7105. The wide range of Sr values indicate more than one Sr-source. The Sr-isotope composition of country rock and local intrusive samples also vary widely and the sources of the Sr present in the vein cannot be determined unequivocally.

Stable isotope data suggests two fluids were involved in the mineralizing process, an exchanged meteoric fluid and a magmatic fluid. Calcite derived δD values (-61 to -37‰) are heavier than quartz derived δD values (-82 to -52‰). This data in conjunction with the oxygen isotope data (calcite $\delta^{18}O_{H_2O}$ = 0.6 to 8.3‰ and quartz $\delta^{18}O_{H_2O}$ = 4.1 to 9.4‰) suggest that these minerals may have been precipitated by two mixing fluids in which calcite and quartz are associated predominantly with exchanged meteoric and magmatic components, respectively.

The $^{87}Sr/^{86}Sr$ composition of vein calcites have a strong inverse correlation with $\delta^{13}C$ and a lesser one with $\delta^{18}O$. These relationships are most likely the result of the mineralizing fluids interacting with the host rocks. No relationships were evident between the quartz and calcite data and the stage of mineralization (i.e. time) and the host rocks, except for the $^{87}Sr/^{86}Sr$ values of the stage IV calcites which fall in a very narrow range compared to the widely varying values of the other stages.

The gases from quartz-hosted fluid inclusions were analyzed from bulk samples. Oxygen and sulfur fugacities were determined using the gas data. Oxygen fugacities have a small range of values (log f_{O_2} = -42.5 to -39.8) and appear to be buffered by carbon-rich wall rocks. Sulfur fugacities vary widely. Regions of lower fluid inclusion Th and higher salinities reported in Querol *et al.* (1989) coincide with regions of higher H_2S concentrations in fluid inclusions. Factor analysis of gas data indicates the partitioning of gases into a vapor phase during boiling. A second factor suggests the addition of a higher salinity, H_2S-rich fluid to the mineralizing system. A combination of boiling and mixing with a lower salinity fluid resulted in the observed oxygen and sulfur fugacities. However, both low and relatively high salinities are reported for quartz-hosted fluid inclusions (Simmons *et al.*, 1988) which maybe the result of mixing and/or two magmatic fluids, one dilute and one saline. Both sets of conditions could produce the observed stable isotope values in which each stage represents a pulse of high salinity, H_2S-rich fluid which either became more diluted by mixing with a lower salinity magmatic fluid and a meteoric fluid or by mixing with a meteoric fluid alone.

ACKNOWLEDGEMENTS

I am grateful to the management of Compania Fresnillo, S.A. de C.V., for the opportunity to do this project. I would like to thank the geological and exploration staff of the Fresnillo mine for their guidance, support, and hospitality during my stay at the mine. In addition, Dr. Francisco Querol provided timely discussions on the data. I would also like to thank Drs. Dave Norman and Andrew Campbell for their help in the formation and execution of this project which would not have been possible without the generous support of the stable isotope laboratory of Dr. Andrew Campbell and the quadrupole mass spectrometry laboratory of Dr. David Norman at New Mexico Institute of Mining and Technology and the geochronology laboratory of Dr. Doug Brookins at the University of New Mexico at Albuquerque. The assistance and advice of David Ward on strontium isotope analytical procedures is gratefully acknowledge. Many of the nicely drawn figures are the work of John Lucio; who generously allowed me to use them. This project was partially funded by the Geological Society of America and Mineral Institute of New Mexico Institute of Mining and Technology grant number G1184135.

TABLE OF CONTENTS

LIST OF FIGURES

LIST OF TABLES

INTRODUCTION

The ore deposits of the Fresnillo district have been a significant source of silver since the discovery of the Proaño vein in 1553 (Bargalló, 1955). Over 10,000 tons (metric) of Ag, 15 tons of Au, and 500,000 tons of both Pb and Zn have been extracted from the Fresnillo mines (García *et al.*, 1989). The ore mineralization of the district exhibit various styles consisting of mantos, chimneys, stockworks, veins, and disseminated ore bodies. The genesis of the ore deposits remains unclear after numerous studies on the district, some of the most notable being Stone and McCarthy (1948), Koch and Link (1967), de Cserna (1976), Kreczmer (1977) Macdonald (1978), Chico (1986), Albinson (1988), Lang *et al.* (1988), Ruvalcaba-Ruiz and Thompson (1988), and Lucio (1990). One of the ore bodies, the silver-rich Santo Niño vein, has been the subject of several recent studies (Gemmell, 1986; Simmons, 1986; Benton, 1987; Gemmell *et al.*, 1988; Simmons *et al.*, 1988; Gemmell *et al.*, 1989). Despite this intense study, certain questions about the genesis of the vein remain unanswered.

This study attempts to address two questions regarding vein genesis: (1) where do the components of the mineralizing solutions originate; and (2) how do they evolve during the mineralizing process? These questions are examined using stable isotopes, Sr isotopes, and quantitative analysis of fluid inclusion gases on material that has been studied in detail by others (Gemmell, 1986; Simmons, 1986; Gemmell *et al.*, 1988; Simmons *et al.*, 1988; Gemmell *et al.*, 1989). The stable isotopes are used to investigate the source of the hydrothermal fluids. Strontium isotopes are used to trace the source of solutes in the fluids. Fluid inclusion gases are analyzed to indirectly access the physical and chemical changes of the ore depositing fluid. In conjunction with other data, these techniques have been used to study the hydrothermal system responsible for the Santo Niño vein.

DISTRICT GEOLOGY

Introduction

The Fresnillo district is located on the western margin of the Mesa Central near the western edge of the Sierra Madre Occidental (Fig. 1). Mineralization occurs in a thick sequence of Cretaceous marine sedimentary rocks and submarine volcanics overlain unconformably by Tertiary continental sediments and felsic volcanics (de Cserna, 1976; Vallejo, 1983). In the district, a quartz monzonite, granodiorite, and quartz trachyte intrude the Cretaceous sediments and rhyolite dikes cross cut the lower and middle-portions of the Tertiary volcanic sequence (Fig. 2).

Stratigraphy

The Early Cretaceous Proaño Group is the oldest known unit in the district and is subdivided into the older Valdecañas and the younger Plateros Formations. A marine origin has been established for this thick sedimentary sequence of greywackes and shales based on fossil evidence and lithology (de Cserna, 1976; Davila Alcocer, 1981).

The Valdecañas Formation, or lower greywacke, is observed only in the underground workings of the mine and may be over 1000 m thick (Simmons, 1985). It is a rhythmic sequence of thinly bedded, light greenish-gray greywacke interbedded with thin beds of medium to dark gray carbonaceous shales, with discontinuous beds and lenses of dark gray micrite (de Cserna, 1976; Simmons, 1985).

The Plateros Formation, or upper greywacke, conformably overlies the lower greywacke. The lower portion, called the lutite by the mine staff, consists of a 150 to 300 m thick sequence of carbonaceous and calcareous shales. It is conformably overlain by a 200 to 500 m sequence of alternating dark to greenish gray greywackes and shales interbedded with thinner units of dark gray to black carbonaceous shales (de Cserna, 1976; Davila Alcocer, 1981; Vallejo, 1983; Simmons, 1985). The Proaño Group is conformably

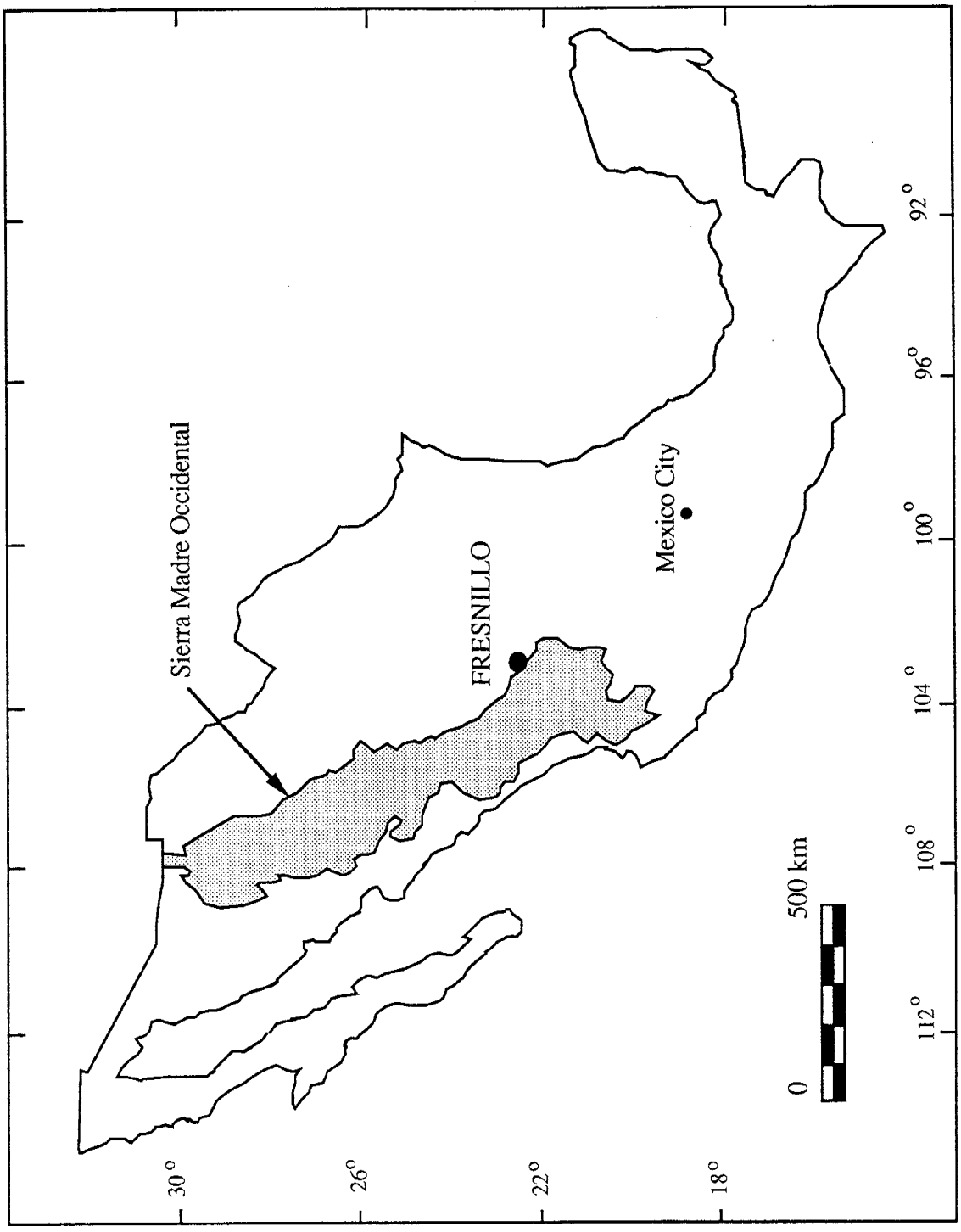

Figure 1. Location map of the Fresnillo district, Zacatecas, Mexico (After Campa and Coney, 1983; Gemmell, 1986).

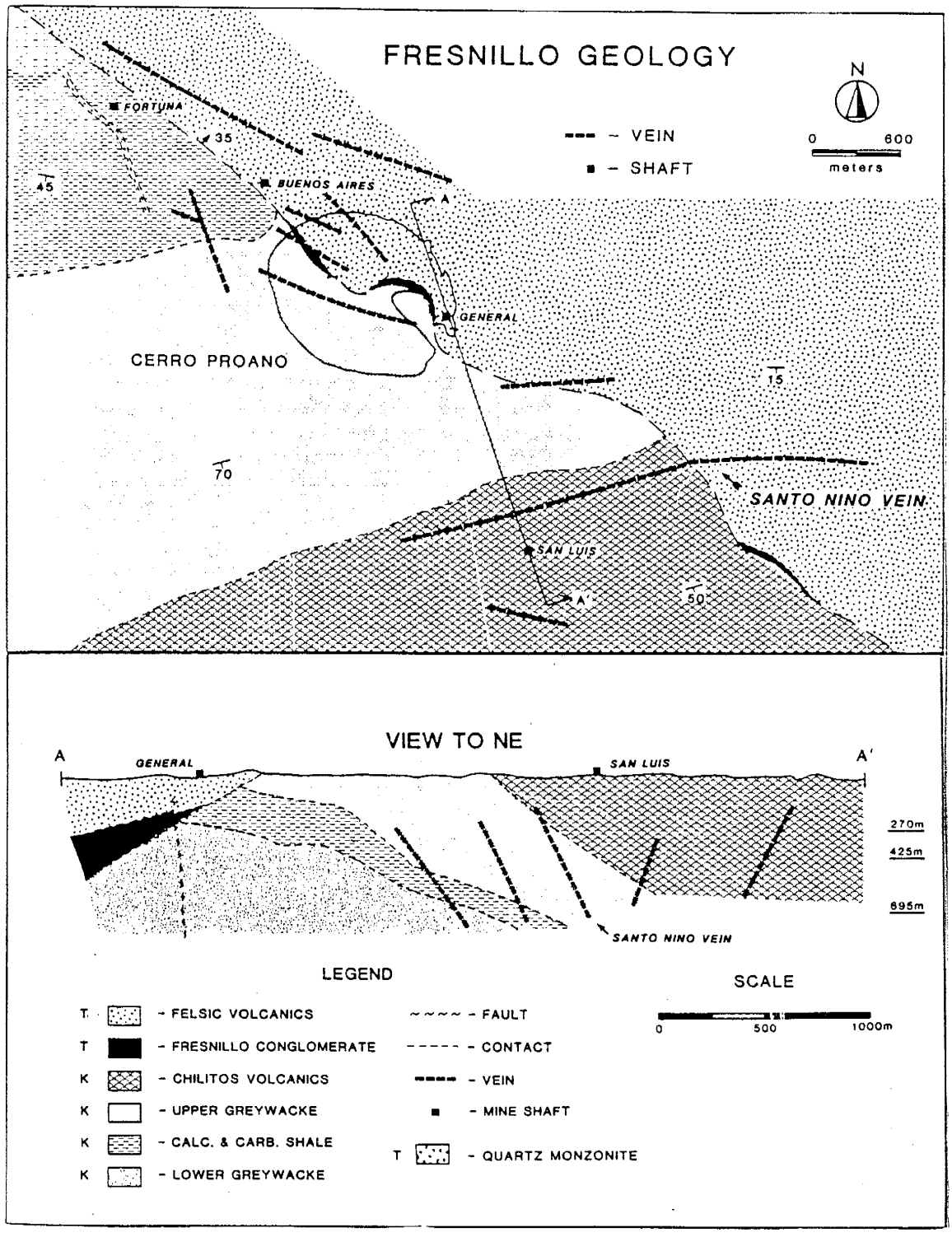

Figure 2. Simplified geologic map and cross-section of the Fresnillo district geology in the vicinity of the mine. T=Tertiary, K=Cretaceous (From Gemmell *et al.*, 1988).

overlain by the Chilitos Formation. It consists of a sequence of basaltic to andesitic flows and pillow lavas interbedded with shales, greywackes, lenses of marls and micritic limestones, and laharitic-type volcanic epiclastic rocks (de Cserna, 1976; Vallejo, 1983; Simmons, 1985; Gemmell, 1986) between 200 m (de Cserna, 1976) and 375 m thick (Querol, 1980).

The Fortuna Limestone and the Cerro Gordo Limestone are present in the district, but not in the vicinity of the mine. The former is a 500 m sequence (de Cserna, 1976) of thinly to medium-bedded, dark gray carbonate rocks. The latter is a 300 m sequence of compositionally similar medium- to thickly bedded rocks.

The Fresnillo Formation unconformably overlies the Chilitos Formation and ranges in thickness from 0 to 300 m. It is a conglomeritic unit that grades upward into arkosic sediments and felsic tuffs. The conglomerate is composed of unsorted, angular to subangular clasts of greywacke, limestone, shale, chert, and quartz in a matrix of sand and minor silt (de Cserna, 1976; Vallejo, 1983).

A thick volcanic sequence conformably overlies the Fresnillo formation and is estimated to be greater than 500 m thick (Vallejo, 1983; Gemmell, 1986). It consists of felsic lavas, tuffs, and pyroclastic flows which are overlain by a small unit of olivine basalt flows (Simmons, 1985). This volcanic sequence has been correlated with other Late Eocene to Oligocene pyroclastic deposits present throughout the Sierra Madre Occidental (Gemmell, 1986). The basal unit, a welded tuff, and uppermost felsic unit, a porphyritic rhyolite flow, have whole rock K-Ar ages of 38.3 $\pm$ 0.8 Ma and 27.5 $\pm$ 1.2 Ma, respectively (Lang *et al.*, 1988). Quarternary alluvium is found as thin deposits in drainage areas up to a thickness of 30 m (Simmons, 1985). In addition, deposits of caliche, up to 20 m in thickness, cover many of the slopes in the district (Gemmell, 1986).

Intrusive Rocks

A small quartz monzonite stock/dike intrudes the lutite and upper greywacke units

in the western portion of the mine. It is exposed 150 m southwest of Tiro Fortuna (Fig. 3) and in the underground workings of the Fortuna area (Gemmell, 1986). Alteration obscures the spatial relationships of the mineralization and the intrusive (Kreczmer, 1977). However, Kreczmer (1977) uses mineralogical evidence to propose that the intrusive predates mineralization. A whole rock K-Ar date of 32.4 ± 0.8 Ma obtained from the stock has been proposed as a minimum age for the intrusion (Lang *et al.*, 1988).

A small amount of porphyritic granodiorite is exposed intruding into the Cretaceous shales and limestones north of the town of Plateros. The intrusive body exhibits varying degrees of hydrothermal alteration associated with crosscutting quartz-sulfide veins (Simmons, 1986). A whole-rock K-Ar date obtained from material reported to have very minor hydrothermal alteration by Lang *et al.* (1988) suggests a minimum age of 32.9 ± 0.7 Ma for the intrusion.

A light brown quartz trachyte intrudes the Cretaceous sediments southwest of Plateros and is postulated by Simmons (1986) to be from an intrusive at depth. A whole-rock K-Ar age of 33.5 ± 0.8 Ma is reported for the intrusion (Lang *et al.*, 1988). In addition, several dark brown rhyolite dikes are exposed 7.5 km southeast of Cerro Proaño. They intrude the Cretaceous sediments into the middle of the Tertiary volcanic sequence and are considered to be feeders to the overlying pyroclastic flows (de Cserna, 1976). Stratigraphic relations suggest an Oligocene age for the dikes (Gemmell, 1986). A number of small (1 m thick) meta-granodiorite dikes intrude the sediments of the Proaño Group and the andesites of the Chilitos Formation (Gemmell, 1986); these have not been dated.

Structure

The first major structural event recorded in the rocks of the Fresnillo district occured in the Late Cretaceous during which pre-Tertiary units were subjected to strong compressional forces associated with the Laramide orogeny. This resulted in folding and thrust faulting (Campa, 1985). A broad anticlinorium that plunges gently to the southeast

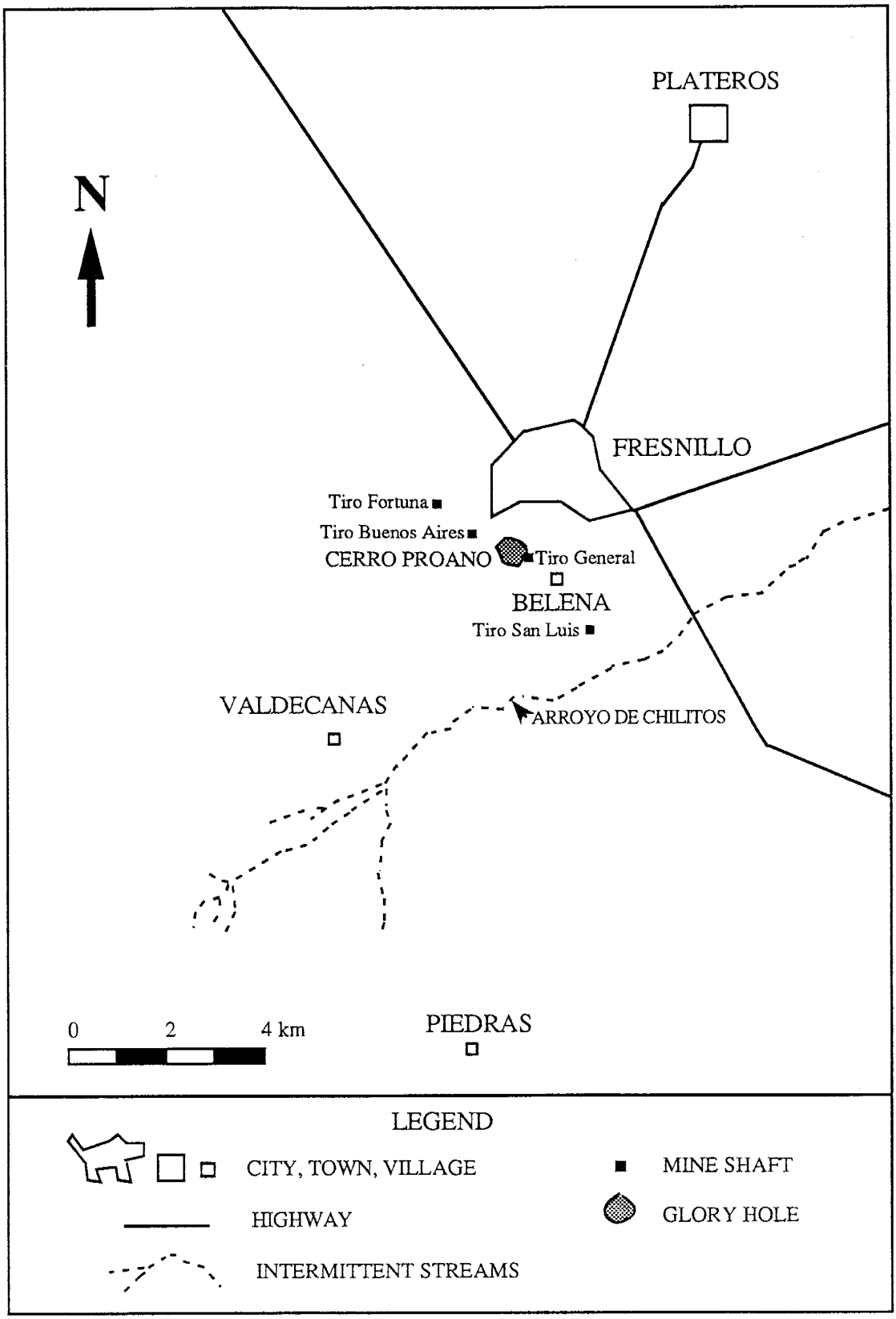

Figure 3. Index map of the cities, towns and villages of the Fresnillo district. The mine shafts of the Fresnillo mine are shown (From Lucio, 1990; After Gemmell, 1986).

beneath Cerro Proaño reveals crumpling and contorting of the Proaño Group sediments by this event (Stone and McCarthy, 1948; Gemmell *et al.*, 1988). A second event occured in the Middle to Late Tertiary during which tensional stresses produced block faulting (Simmons, 1986). The Fresnillo fault is associated with this deformation and has a throw of at least 300 m. Extensive minor tensional faulting and fracturing followed these events occuring contemporaneously with the hydrothermal activity associated with mineralization of the Santo Niño vein (Gemmell, 1986; Simmons, 1986).

Ore Deposits

The ore bodies of the Fresnillo mine are encompassed by a 5 km long, 1 to 2 km wide zone, roughly centered on Cerro Proaño (Fig. 4). A variety of styles of ore mineralization are observed including stockworks, veins, mantos, chimneys, and disseminated ore that have been mined to a depth of 1100 m (Chico, 1986). Based on fluid inclusion evidence, the chimneys, mantos, and deeper veins are postulated to have formed at temperatures between 305° and 415°C, whereas stratigraphically higher silver-rich veins are reported to have formed at temperatures less than 320°C (Ruvalcaba-Ruiz and Thompson, 1988).

Mineralization from the surface to 100 m depth occurs as oxidized stockworks covering an area of 700 m by 200 m on Cerro Proaño (Lowther, 1981). Mining was conducted from 1921 to 1943 by the glory-hole method yielded 13 million tons of ore with grades of 0.3 g/ton Au and 190 g/ton Ag. Since 1927, nearly all production has been from sulfide mineralization which begins about 100 m below the top of Cerro Proaño (Stone and McCarthy, 1948). The important sulfide mineralization consists of pyrite, sphalerite, galena, arsenopyrite, tetrahedrite, and pyrargarite, with lesser amounts of polybasite, argentite, pyrrhotite, and matildite. Quartz and calcite are the predominant gangue minerals (Simmons, 1986).

The replacement ore bodies at Fresnillo occur in the Fortuna and Tiro General

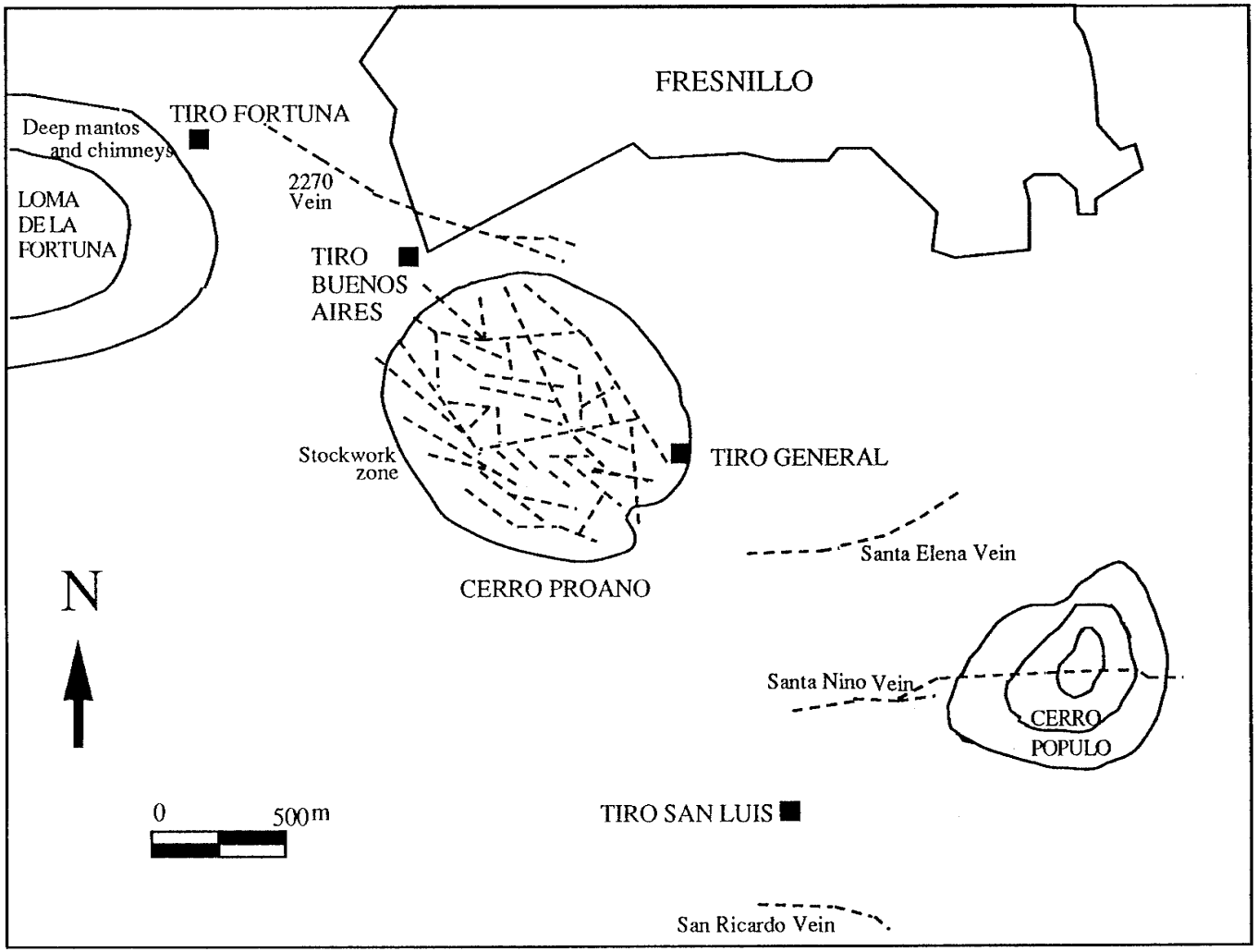

Figure 4. Generalized index map of the ore deposits of the Fresnillo district (From Lucio, 1990; After Ruvalcaba-Ruiz, 1980).

areas of the mine. The Fortuna area is located approximately 1.5 km northwest of Cerro Proaño (Fig. 4) between the 830 and 1030 m levels of the mine covering an area of 70,000 m^2. Here, replacement mineralization occurs as mantos and chimneys hosted predominantly by thin interbedded shales and greywackes of the lower greywacke near the quartz monzonite intrusion. The Tiro General section, located beneath Cerro Proaño, has both manto and the disseminated ore bodies between the 385 and 470 m levels and the 105 and 270 m levels, respectively (Chico, 1986). A magmatic origin of the fluids has been proposed by MacDonald *et al.* (1986) based on S-isotopic data for sulfides from the deep mantos.

Nearly 100 veins and veinlets are known in the Fresnillo area. However, only 10 can be considered major veins. The veins are divided according to mineralogy into light sulfide veins rich in Ag, with Pb and Zn and heavy sulfide veins rich in Pb and Zn with significant amounts of Ag (Stone and MacCarthy, 1948). Light sulfide veins are characterized by quartz and calcite gangue with silver sulphosalts, and variable amounts of galena, sphalerite, chalcopyrite, and pyrite. The Santo Niño, Santa Elena, San Ricardo, 2270, Esperanza, Agripo, and additional minor veins are in this group. Heavy sulfide veins are characterized by comparatively less quartz and calcite and large amounts of base-metal sulfides with increasing pyrrohtite and arsenopyrite with depth (Stone and McCarthy, 1948; Koch and Link, 1967). Veins in this group are the Cueva Santa, 2137, 2137FW, 2200, 1600, Plomosa, and almost all the veins of the Tiro General section of the mine (Chico, 1986).

Alteration

Alteration styles identified in the Fresnillo district include silicic, propylitic, argillic, phyllic, and potassic alteration. The alteration associated with the Cretaceous units is poorly developed and restricted to the areas immediately adjacent to veins and mantos (Simmons, 1986). For the silver-rich veins, the alteration is irregular and limited to narrow

adjacent zones. Veinlets that offshoot the main veins commonly show no evidence of related alteration (Ruvalcaba-Ruiz and Thompson, 1988). Sediments proximal to the quartz monzonite stock in the Fortuna area of the mine have been extensively silicified, almost to the point of a monomineralic composition. Greywackes in the vicinity of Cerro Proaño and Tertiary volcanics near Fresnillo and Piedras have also been subjected to varying degrees of scilicic alteration (Ruvalcaba-Ruiz and Thompson, 1988). Argillic alteration is characterized by kaolinite and montmorillonite with variable pyrite and minor halloysite, sericite, chlorite, and epidote. The width of the argillic alteration associated with the veins varies from 0.05 to 10 m (Ruvalcaba-Ruiz and Thompson, 1988). Intense argillic alteration is associated with the lower and middle Tertiary volcanics units near Piedras and is attributed to hot springs activity (Simmons, 1986). Phyllic alteration is characterized by sericite and pyrite with minor illite, kaolinite, and montmorillonite. This style of alteration is more pronounced in rocks with relatively higher abundances of K-feldspar such as the immature sands of the lutite. Phyllic alteration halos extend out 0.01 to 1 m from the associated silver-rich veins. Potassic alteration is relatively rare and is characterized by the formation of adularia. It has been observed only in the Santo Niño vein and adjacent wall rocks. Adularia in the wall rocks has been partially altered to sericite (Ruvalcaba-Ruiz and Thompson, 1988).

Propylitic alteration is the most widespread style of alteration in the Fresnillo district. It is characterized by calcite, epidote, and chlorite with minor pyrite. Variable amounts of montmorillonite and kaolinite also occur depending on the alteration intensity and the host rock composition. Propylitic alteration exists adjacent to the veins when it is the sole alteration present and up to 4 m away from the vein when associated with other kinds of alteration (Ruvalcaba-Ruiz and Thompson, 1988). The extensive propylitic alteration associated with the Chilitos Formation andesites is believed to be primarily due to syndepositional alteration (Simmons, 1986). Petrographic and trace element analyses of Cretaceous sediments collected from the drift between Tiro General and Tiro San Luis on

the 425 m level of the mine by Lucio (1990) indicate evidence of propylitic alteration. Trace element analyses show an increase in Na, Mg, Ca, P, and Mn in altered samples compared to an upper greywacke sample obtained 2 km northwest of Plateros which is reported to be unaltered. However, Ruvalcaba-Ruiz and Thompson (1988) report no evidence of alteration apparent in the shaley material of the calcareous lutite when cut by silver-rich veins, but moderate propylitic alteration is evident in immature sands of this unit.

Age of hydrothermal activity

Clark *et al.* (1982) suggest that the Pb-Zn-Ag deposits of northern Mexico were formed between 49-26 Ma during late arc progression and early regression. Radiometric dating of hydrothermal products agree with this timing. K-Ar ages determined for hydrothermal K-feldspar from the Piedras hot springs deposit and intensely sericitized material from Plateros constrain hydrothermal activity to 29-31 Ma in the Fresnillo district. Cross-cutting relationships also constrain the timing of hydrothermal activity. Ag-rich veins in the southeastern portion of the district are hosted by both the Late Eocene-Early Oligocene Fresnillo Formation and the overlying ignimbrite which has a whole rock K-Ar age of 38.4 ± 0.8 Ma (Lang *et al.*, 1988). Fresh volcanics overlying hydrothermally altered rocks in the Sierra de Valdecañas have whole rock K-Ar ages of 27.4 ± 1.5 and 27.7 ± 0.6 Ma indicating the end of hydrothermal activity (Lang *et al.*, 1988).

SANTO NIÑO VEIN

The Santo Niño vein was discovered in 1975 and has been a major ore producer for the Fresnillo mine in recent years. It is over 2.5 km long and the width pinches and swells from 10 cm to 4 meters, but averages less than 2.5 m (Simmons, 1986). Most of the vein is hosted by the upper greywacke and the Chilitos Formation, except for the eastern end

where it crosscuts the Fresnillo fault and is situated in the Fresnillo Formation and overlying tuffaceous rhyolite. In September 1985, the ore extracted from the vein had an average grade of 770 g Ag/metric ton (Simmons, 1986). However, silver grades do exceed several kg/ton locally.

The Santo Niño vein has been the focus of several detailed studies. Ruvalcaba-Ruiz (1980) studied the geology and alteration and conducted a limited fluid inclusion study. Gemmell (1986) meticulously examined the vein stratigraphy, mineralogy, and structure. In a companion study, Simmons (1986) did a detailed fluid inclusion study which has been supplemented by Querol *et al.* (1989). These studies report fluid inclusion homogenization temperatures (Th) ranging from 180° to 260°C and are considered trapping temperatures due to evidence of fluid boiling. Apparent fluid inclusion salinities range from 2 to 12.5 equivalent weight percent NaCl (eq. wt. % NaCl) and fall into two distinct populations indicating a system with pulses of a high salinity fluid alternating with a lower salinity fluid. Additionally, Th values are inversely related to salinities. Simmons (1986) also conducted a study of helium, hydrogen (δD), and oxygen ($\delta^{18}O$) isotopes. The $\delta^{18}O$ and δD are interpreted to be characteristic of a meteoric water that had undergone extensive water/rock interaction, and may include mixing with a magmatic water with the addition of a metamorphic fluid toward the end of mineralization. Helium isotope values range from 1.16 to 2.1 times the present-day atmospheric value, indicating the presence of diluted mantle He. These values were interpreted to suggest that the magma from which the He originated could have been the source of other volatile components (e.g. Cl_2, H_2S, and CO_2) necessary for ore genesis. Lucio (1990) examined the Pb isotopes of the district, concluding that the metals in the ore bodies had a common, homogeneous source that cannot be identified unequivocally. He concluded the most likely sources of the lead was from leaching of the Cretaceous sediments or injection of metalliferous magmatic fluid from melts associated with younger volcanics. Benton (1987) investigated trace element and Sr-isotope composition of vein calcites. The results indicated that Fe, Mn, and Mg

concentrations in the vein calcites were closely related to the proposed direction of fluid flow within the vein reported by Gemmell (1986). The strontium isotope data was inconclusive.

Mineralogy and stratigraphy

Four stages of mineralization have been identified for the Santo Niño vein by Gemmell (1986) and Gemmell *et al.* (1988). They are interpreted to represent a mineralogical record of the multiple fissure openings that allowed hydrothermal fluids to enter the areas of mineralization.

Stage one is the most important ore producing stage. It is characterized by crackle, fragment-supported, and matrix-supported breccias. Cockade banding is well developed around 1 to 25 cm fragments. Bands are composed of thin layers quartz, calcite, and sulfides such as pyrite, sphalerite, galena, and pyrargarite. The breccias are cemented by a matrix of white to gray massive quartz with late stage minor amethyst and calcite. Stage two is characterized by a breccia that grades into a hanging-wall crackle breccia. Fragments are predominantly 2 to 10 cm fragments and cockade banding is poorly developed. Mineralization consists of quartz with minor sulfides followed by late calcite. Stage three consists of well developed symmetrical crustiform banding. This ore-producing stage consists of pyrite, sphalerite, galena, pyrargerite, gray and white quartz, and minor amounts of chalcedony, amethyst, and calcite. Stage four is almost devoid of sulfides and occurs as massive, coarsely crystalline white calcite with trace amounts of fine-grained, disseminated pyrite and rare blebs of amethyst.

Alteration

Hydrothermal alteration associated with the Santo Niño vein is limited in development and is restricted to areas immediately adjacent to the vein (Gemmell *et al.*, 1988). Host-rock breccia fragments within the vein exhibit varying degrees of argillic and

silicic alteration. Simmons *et al.* (1988) states that altered fragments commonly coexist in the vein with unaltered fragments of similar size and lithology.

ANALYTICAL METHODS

Strontium isotopes

Strontium isotope ratios were measured in vein calcite; quartz hosted fluid-inclusion waters; local intrusives; and sedimentary and igneous rocks which host and overlie the Santo Niño vein. Whole rock and calcite samples were prepared using conventional methods modified from Ward (1990). Quantitative analysis of Rb and Sr in whole rock samples was obtained by X-ray fluorescence. Rubidium concentrations were measured for two calcite samples by isotope dilution. The Rb and Sr concentrations of the fluid inclusion waters were also determined by isotope dilution.

Samples used for Sr-isotope analysis of fluid-inclusion waters were scrupulously cleaned prior to analysis using methods modified from Roedder (1958; 1963), Norman (1978), and Bottrell *et al.* (1988). Fluid inclusion components were liberated by thermal decrepitation of 10 to 12 g of material in quartz flasks (Norman, 1978; Norman and Landis, 1983). This process was carried out under vacuum allowing the fluid inclusion waters to be collected for hydrogen isotope analysis. The quartz and evolved salts were then leached with a 1 percent purified HNO_3, 200 ppm $LaCl_3$ solution. The leachate was then dried and rehydrated with 2 ml of 6 *N* HCl, and dried again. After cation separation and final sample preparation, the samples were run on a VG235 solid source mass spectrometer at the laboratory of Dr. D. Brookins at University of New Mexico, Albuquerque. Repeat analysis of E&A $SrCO_3$ and an inhouse standard suggest an external precision of $\pm$ 24 ppm (1σ, degrees of freedom (n) = 10), while E&A $SrCO_3$ gave a value of 0.708023 $\pm$ 18 ppm (1σ, n = 4). Background levels are 13 $\pm$ 1 ng Sr and 2 $\pm$ 3 ng Rb for a quartz blank prepared and analyzed according to the methods described above. Additional details of sample preparation are presented in Appendix A.

Stable isotopes

A portion of the quartz prepared for Sr-isotope analysis was separated and crushed to a coarse powder for O_2 extraction by conventional methods with a ClF_3 reagent, followed by quantitative conversion to CO_2 (Borthwick and Harmon, 1982; Taylor and Epstein, 1962). Carbon dioxide was extracted from calcite by reaction with 100% H_3PO_4 at 25°C (McCrea, 1950). Fluid inclusion waters liberated from quartz and calcite by thermal decrepitation were converted to H_2 by reaction with a Zn reagent at 470°C for 30 minutes (Coleman *et al.*, 1982). Detailed stable isotope analytical procedures are in Appendix B.

Stable isotope ratios were measured at the laboratory of Dr. A.R. Campbell at New Mexico Institute of Mining and Technology on a FinneganMAT Delta E, gas source mass spectrometer and are reported as δ values in per mille (‰) relative to a standard. For example, oxygen is reported as follows:

$$\delta^{18}O = \frac{^{18}O/^{16}O_{sample} - {}^{18}O/^{16}O_{SMOW}}{^{18}O/^{16}O_{SMOW}} \times 1000‰$$

Analysis of the quartz standard NBS-28 gave a value of 9.7 ± 0.1‰ (2σ), calcite standards, NBS-18, -19, and -20, give a long term variation of ± 0.2‰, and water standards, Standard Mean Ocean Water (SMOW), Greenland Ice and Snow Precipitation (GISP), Standard Light Antarctic Precipitation (SLAP), and an inhouse distiled water, yield variations of ± 4‰. Oxygen and hydrogen isotope values are reported with respect to SMOW and carbon isotope values ($\delta^{13}C$) are reported relative to Pee Dee Formation Belenmite Calcite (PDB).

Quantitative gas analysis

Material used for gas analysis are splits of the quartz prepared for Sr-isotopes analyses. Gases were liberated by thermal decrepitation of 1.0 to 2.5 g of quartz using methods described in Norman and Sawkins (1987). Water and gas pressures were measured with a precision of ± 3% (Norman and Sawkins, 1987). The internal precision of the mass spectrometer is ± 5%. Shepard *et al.* (1985) and Norman and Sawkins (1987) report that thermal decrepitation causes quantitatively insignificant compositional changes in the liberated volatiles. Appendix C addresses the analytical methods of gas analyses in detail.

RESULTS

Strontium-isotope data

Strontium-isotope ratios were measured for 16 samples of quartz-hosted fluid-inclusion solute and 15 samples of calcite selected across the vertical and horizontal extent of the Santo Niño vein (Fig. 5). In addition, 6 strontium isotope analyses of vein calcite are available from Benton (1987). The $^{87}Sr/^{86}Sr$ ratios measured for the fluid-inclusion samples have a range of values from 0.7069 to 0.7090 with the exception of sample FR-88-56 from the 695 m level which has a value of 0.7130. Ratios were corrected for decay since mineralization 30.0 Ma, assuming closed system behavior. Age corrected $^{87}Sr/^{86}Sr$ values range from 0.7064 to 0.7078 with FR-88-56 equal to 0.7105 (Table 1, Fig. 6).

Strontium from both primary and secondary inclusions is liberated during the thermal decrepitation process. No quantitative assessment of fluid inclusion type was made. However, microscopic inspection of several samples indicated secondary inclusions are small and infrequent. Regardless, the contribution of Sr from secondary inclusions may be significant in some cases.

Vein calcites have a wider range of $^{87}Sr/^{86}Sr$ ratios than the fluid-inclusion derived values from 0.7060 to 0.7091 (Table 2). The Rb concentration of two calcite samples, FR-88-15 and FR-88-29, were measured in order to determine if corrections were necessary

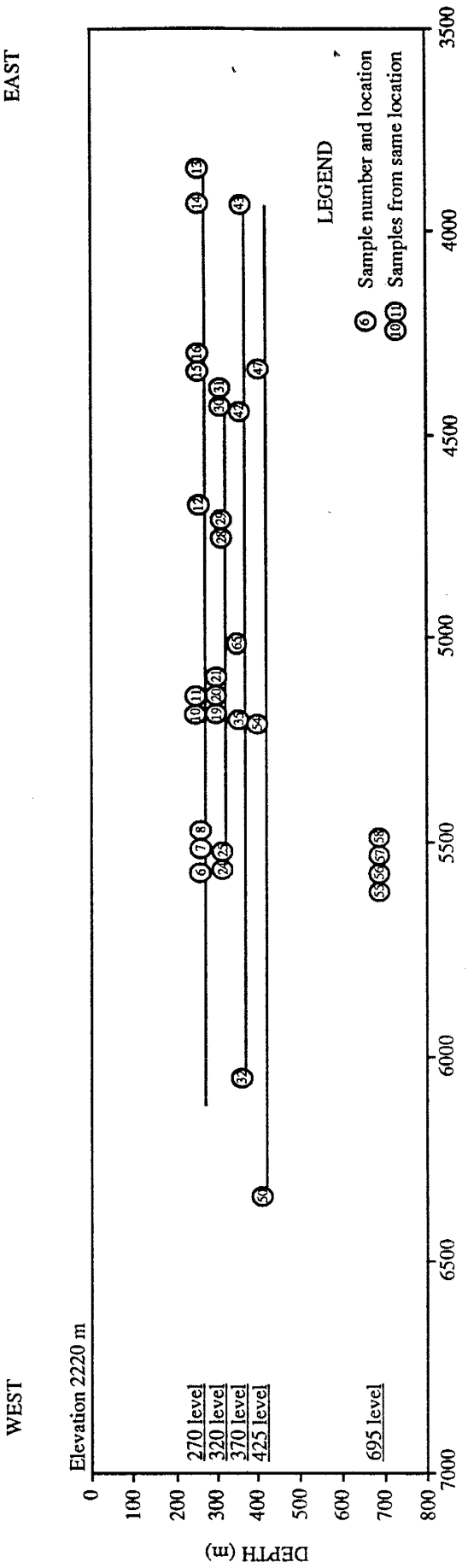

Figure 5. Sample locations within the Santo Niño vein. Longitudinal section N75°W.

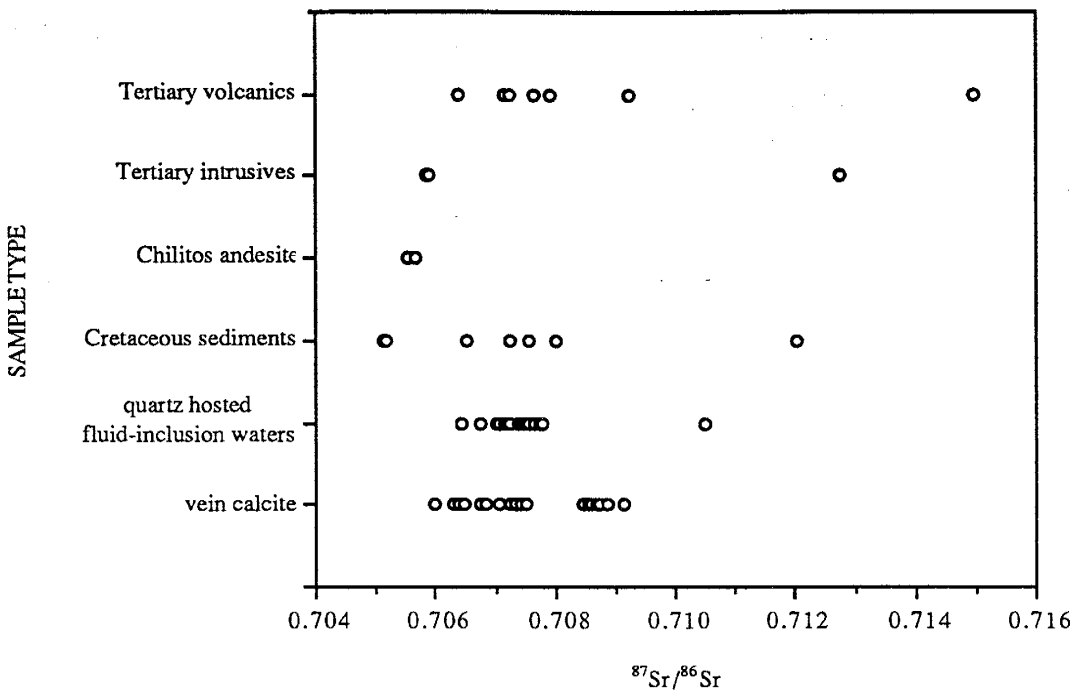

Figure 6. Distribution of Sr-isotope ratios for the different sample types.

TABLE 1. Quartz-hosted fluid-inclusion solute Sr-isotope data

Sample	Stage	Rb (ng)	Sr (ng)	$^{87}Sr/^{86}Sr$ (measured)	$^{87}Rb/^{86}Sr$	$^{87}Sr/^{86}Sr$ (30.0 Ma)
FR-88-7	III	63	505	0.70704 ± 1	0.360	0.70769
FR-88-10	II	44	525	0.70729 ± 4	0.243	0.70719
FR-88-11	I	202	1560	0.70754 ± 1	0.375	0.70738
FR-88-14	II	207	395	0.70828 ± 4	1.517	0.70763
FR-88-16	I	1708	1117	0.70897 ± 3	4.425	0.70709
FR-88-20	II	318	1420	0.70742 ± 4	0.648	0.70714
FR-88-21	III	153	923	0.70746 ± 3	0.479	0.70726
FR-88-24	I	42	314	0.70754 ± 3	0.389	0.70737
FR-88-25	II	194	2971	0.70653 ± 3	0.189	0.70645
FR-88-29	III	134	207	0.70859 ± 3	1.866	0.70779
FR-88-31	II	228	858	0.70782 ± 3	0.769	0.70749
FR-88-47	II	35	467	0.70713 ± 4	0.215	0.70704
FR-88-50	III	383	636	0.70856 ± 1	1.744	0.70781
FR-88-54	III	121	930	0.70768 ± 3	0.378	0.70752
FR-88-56	I	890	437	0.71300 ± 5	5.891	0.71049
FR-88-65	III	571	561	0.70881 ± 3	2.949	0.70755

TABLE 2. Calcite Sr-isotope data

Sample	Stage	$^{87}Sr/^{86}Sr$
FR-88-7	III	0.70638 ± 1
FR-88-8	III	0.70597 ± 1
FR-88-11(a)	I	0.70753 ± 1
FR-88-11(b)	I	0.70709 ± 1
FR-88-12	IV	0.70856 ± 10
FR-88-13(a)	II	0.70711 ± 1
FR-88-13(b)	II	0.70674 ± 1
FR-88-15	I	0.70736 ± 1
FR-88-19	I	0.70744 ± 4
FR-88-28	III	0.70725 ± 1
FR-88-29(a)	IV	0.70887 ± 1
FR-88-29(b)	IV	0.70887 ± 3
FR-88-32	II	0.70861 ± 1
FR-88-35	I	0.70646 ± 1
FR-88-42	IV	0.70870 ± 1
FR-88-55	IV	0.70886 ± 2
FR-88-57	I	0.70876 ± 1
FR-88-58	I	0.70845 ± 1
FR-88-65	III	0.70914 ± 1
16*	IV	0.70868 ± 5
25*	II	0.70741 ± 4
47*	II	0.70729 ± 5
65*	III	0.70702 ± 4
76*	drill core	0.70877 ± 7
89*	II	0.70832 ± 31

*From Benton (1987).

for the decay of ^{87}Rb to ^{87}Sr since mineralization. Both samples contained less than 0.1 ppm Rb. Vein calcites analyzed by Benton (1987) had Sr concentrations averaging 480 ppm. These data indicate that the Rb/Sr ratio is very small at approximately 0.0002. Therefore, the contribution of ^{87}Sr from the decay of ^{87}Rb is probably insignificant for all calcite samples and no correction is necessary.

Replicate analysis of calcite from single crystals were performed on three samples: FR-88-11, FR-88-13, and FR-88-29. The variations in $^{87}Sr/^{86}Sr$ values were 0.00044, 0.00037, and 0.00001, respectively. These compositional differences demonstrate the possible heterogeneity of $^{87}Sr/^{86}Sr$ in the calcites.

Samples for Sr isotope analyses were collected from all known units that may have contributed Sr to the mineralizing fluids, except the Fortuna Limestone and the Cerro Gordo Limestone (Table 3, Fig. 7). These samples included 7 from the Cretaeous sedimentary and volcanic rocks, 9 from the Tertiary sedimentary and volcanic rocks, and 1 each from the quartz monzonite, granodiorite, and quartz trachyte intrusions. In addition, 4 analyses of calcite from the Cretaceous sediments from Benton (1987) and 3 whole rock analyses from the Tertiary volcanics near Piedras from Lucio (1990) are included. All samples, except calcites, were corrected for decay assuming mineralization at 30.0 Ma, except for Tertiary volcanic samples suspected to be syn/post-mineralization which were corrected for decay since formation at approximately 27.5 Ma.

One lower greywacke, 1 upper greywacke , 2 lutite (1 dominated by calcareous material and 1 dominated by shaley material), and 2 samples of calcite from Benton (1987) were obtained from the 425 m level of the mine between Tiro General and Tiro San Luis (Fig. 3). Since rocks in this area have been propylitically altered to some degree according to Lucio (1990), this alteration may have affected the Rb-Sr isotope systematics of the rocks (Farmer and DePaolo, 1987). However, the large range of $^{87}Sr/^{86}Sr$ values obtained for these samples indicates that the original strontium isotope compositions have not been homogenized. Calcite samples appear to be little affected by alteration for the

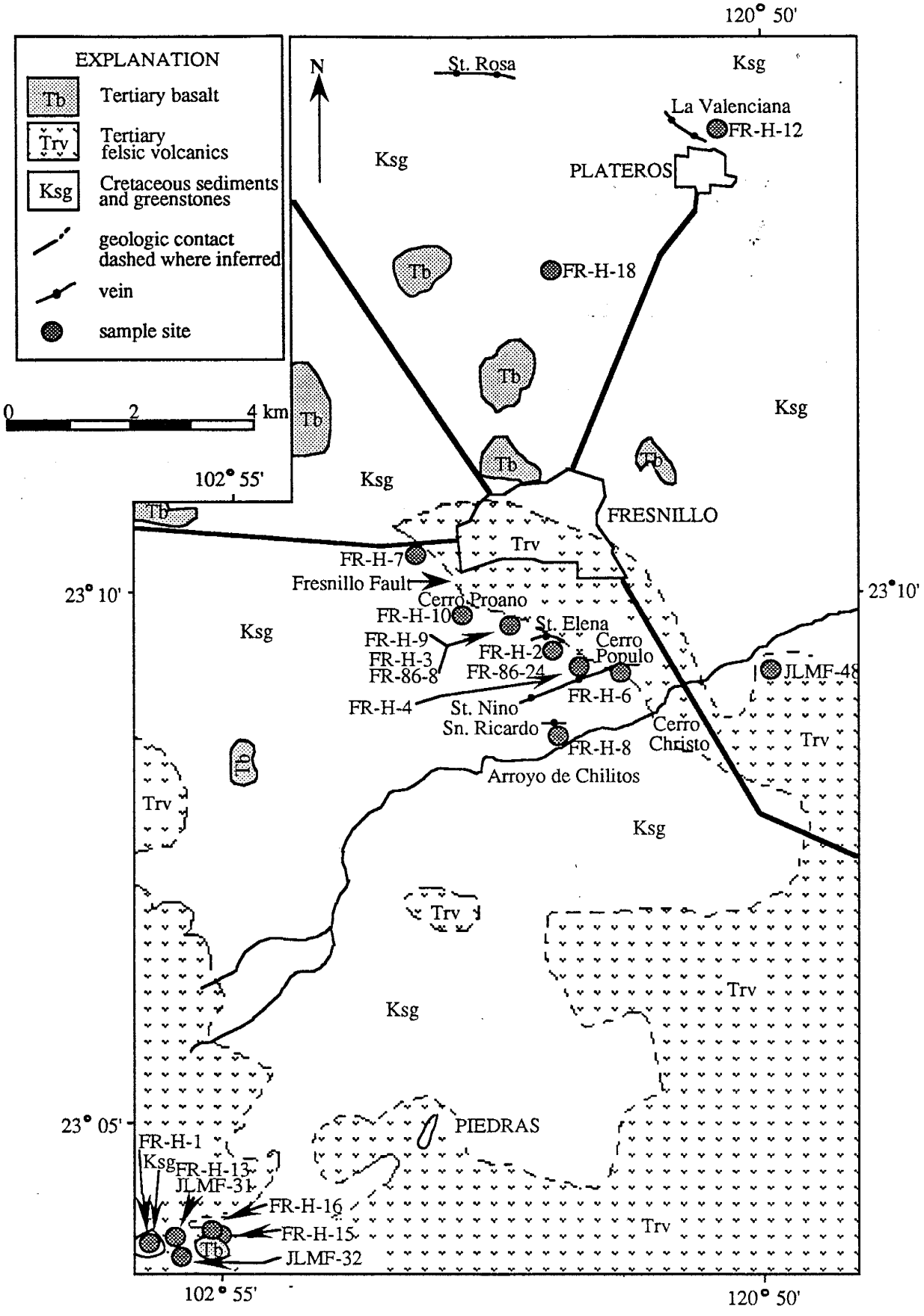

Figure 7. Geologic map of the Fresnillo district with country rock and intrusive sample locations (After Simmons, 1986 and Lucio, 1990).

TABLE 3. Rb, Sr, and $^{87}Sr/^{86}Sr$ Analyses for Fresnillo District Rocks

Sample	Location	Unit	Rb (ppm)	Sr (ppm)	$^{87}Rb/^{86}Sr$	$^{87}Sr/^{86}Sr$ (measured)	$^{87}Sr/^{86}Sr$ (27.5 Ma)
FR-H-13	Piedras	Por rhy flow	301	63	13.742	0.71263 ± 3	0.70726
JLMF-31†	Piedras	Por rhy flow	317	46	19.941	0.71546 ± 4	0.70767
FR-H-15	Piedras	Cryst ignim	273	21	37.791	0.72399 ± 3	0.70923
JLMF-32†	Piedras	Rhy tuff	255	24	30.744	0.72698 ± 4	0.71497
							(30.0 Ma)
FR-H-16	Piedras	Crystal tuff	285	20	41.907	0.72500 ± 2	0.70714
JLMF-48†	Fresnillo	Ignimbrite	207	114	5.254	0.71016 ± 2	0.70792
FR-H-6	Fresnillo	Lwr ignim	137	147	2.694	0.70753 ± 3	0.70639
FR-H-4	Fresnillo	Andesite	214	455	1.361	0.70624 ± 3	0.70566
FR-H-8	Fresnillo	Andesite	191	303	1.822	0.70633 ± 3	0.70555
FR-H-1	Piedras	Chilitos sed	24	308	0.224	0.70661 ± 3	0.70651
FR-H-2	Fresnillo	Upr greyw	98	254	1.116	0.70560 ± 3	0.70513
24*	Fresnillo	Upr greyw	calcite			0.70518 ± 7	
FR-H-3	Fresnillo	Lutite shale	175	86	5.906	0.71455 ± 3	0.71203
FR-H-9	Fresnillo	Lutite calc	45	786	0.167	0.70765 ± 3	0.70758
8*	Fresnillo	Lutite calc	calcite			0.70724 ± 7	
FR-H-10	Fresnillo	Lwr greyw	145	183	2.292	0.70901 ± 2	0.70803
FR-H-7	Fresnillo	Qtz monz	119	371	0.926	0.70629 ± 3	0.70590
FR-H-12	N Plateros	Granodiorite	197	272	2.097	0.70676 ± 3	0.70586
FR-H-18	SW Plateros	Qtz trachyte	90	37	7.106	0.71580 ± 3	0.71277

† From Lucio (1990)
* From Benton (1987)

$^{87}Sr/^{86}Sr$ values are very similar to the whole rock values of corresponding units.

Chilitos Formation samples from the mine and drill core have similar corrected $^{87}Sr/^{86}Sr$ values of 0.7057 and 0.7056, respectively. One sample of greywacke was collected from the Chilitos Formation near Piedras in the Sierra Valdecañas and yielded a corrected $^{87}Sr/^{86}Sr$ value of 0.7065.

The corrected $^{87}Sr/^{86}Sr$ values for Tertiary volcanic rock samples range from 0.7064 to 0.7150. No hydrothermal alteration was evident in the samples analyzed. K-Ar dates of these units indicate the rocks have not been disturbed by hydrothermal solutions. Age dates decrease upwards with volcanic stratigraphy and Fresnillo area units are similar to those found in adjacent areas (Lang *et al.*, 1988).

Quartz monzonite and granodiorite samples have corrected $^{87}Sr/^{86}Sr$ values of 0.70590 and 0.70586, respectively. The similar values suggest that the intrusions may have a common source at depth and that the hydrothermal alteration present either did not affect the Rb-Sr systematics or the fluids were in equilibrium with the intrusive. The quartz trachyte has a relatively radiogenic corrected $^{87}Sr/^{86}Sr$ value of 0.7128.

Stable-isotope data

Oxygen and carbon-isotope results

Nineteen samples of quartz and 16 samples of calcite, representing the horizontal and vertical extent of the Santo Niño vein, were analyzed for oxygen-isotope composition. Quartz $\delta^{18}O$ values ranged from 15.1 to 19.5‰. Calcite $\delta^{18}O$ values had a larger range from 8.6 to 15.8‰. Carbon-isotope compositions for 19 calcite samples range from -8.4 to -3.3‰ (Table 4).

Oxygen-isotope values were calculated to represent $\delta^{18}O_{H_2O}$ using equations from Clayton *et al.* (1972) for quartz and O'Neil *et al.* (1969) for calcite. The temperatures used for the corrections were determined by locating sample positions on contour plot of fluid inclusion Th values from Querol *et al.* (1989) and assuming the value of the intersecting

TABLE 4. Stable isotope data

Sample	Mineral	δD_{H_2O}	$\delta^{13}C_{calcite}$	$\delta^{18}O_{mineral}$	$\delta^{18}O_{H_2O}$	T (°C)
FR-88-6	Quartz	-67		16.4	5.8	215
FR-88-7	Calcite	-61	-3.9	14.1	5.9	216
FR-88-7	Quartz	-52		15.9	5.4	216
FR-88-8	Calcite	-43	-4.6	12.9	4.6	216
FR-88-10	Quartz	-67		16.6	5.6	210
FR-88-11	Calcite†	-64	-5.5	13.7	5.1	210
FR-88-11	Quartz	-64		17.5	6.7	210
FR-88-12	Calcite†	-64	-6.2	15.4	7.1	216
FR-88-13	Calcite†	-59	-6.8	11.9	3.3	209
FR-88-14	Quartz	-66		15.1	4.1	209
FR-88-15	Calcite	-55	-7.0	14.1	5.0	198
FR-88-16	Quartz	-69		17.9	6.2	198
FR-88-19	Calcite†	-72	-6.7	14.1	5.7	212
FR-88-20	Quartz	-66		16.7	5.9	212
FR-88-21	Quartz	-78		17.5	6.7	212
FR-88-24	Quartz	-56		17.1	6.9	222
FR-88-25	Quartz	-69		18.0	7.7	222
FR-88-28	Calcite†	-58	-7.2	15.2	7.5	228
FR-88-29	Calcite	-53	-8.3	15.3	7.6	228
FR-88-29	Quartz	-56		16.6	6.7	228
FR-88-30	Quartz	-67		17.9	6.7	205
FR-88-31	Quartz	-82		16.8	5.6	205
FR-88-32	Calcite†	-58	-6.3	13.4	5.8	231
FR-88-35	Calcite	-37	-4.1	8.6	0.6	221
FR-88-42	Calcite	-40	-7.9	15.3	6.8	210
FR-88-43	Quartz	-72		16.7	6.5	222
FR-88-47	Quartz	-65		16.0	5.2	212
FR-88-50	Quartz	-73		19.5	9.4	225
FR-88-54	Quartz	-62		17.2	7.4	231
FR-88-55	Calcite	-54	-7.3	15.3	7.9	236
FR-88-56	Quartz	-77		15.9	6.5	236
FR-88-57	Calcite†	-68	-7.9	12.5	5.1	236
FR-88-58	Calcite†	-57	-7.5	10.0	2.7	236
FR-88-65	Calcite	-43	-7.8	15.8	7.6	218
FR-88-65	Quartz	-71		17.5	7.1	218

† quartz/calcite mix δD values

isotherm. This procedure assumes that the temperature of the hydrothermal fluid is buffered by the wall rock and the average Th for a certain location is an accurate representation of the temperature at which quartz and calcite precipitated. The $\delta^{18}O_{H_2O}$ values calculated for the quartz and calcite analyzed range from 4.1 to 9.4‰ and 0.6 to 8.3‰ respectively (Fig. 8). For the quartz samples, all but 2 values fall in the narrow range of 5.2 to 7.7‰. Calculated $\delta^{18}O_{H_2O}$ values from quartz are related to temperature, but $\delta^{18}O_{quartz}$, $\delta^{18}O_{calcite}$, and calcite derived $\delta^{18}O_{H_2O}$ values are not.

Hydrogen-isotope results

Fluid inclusion waters from 19 quartz samples, 8 calcite samples, and 8 quartz/calcite mix samples were analyzed for hydrogen-isotope composition. Quartz/calcite mixtures were analyzed in cases when not enough calcite could be separated for δD measurements. The resulting data were corrected to accepted standards including SMOW, GISP, SLAP, and an inhouse standard of distiled water. The quartz, quartz/calcite, and calcite samples yielded corrected δD values ranging from -82 to -52‰, -72 to -42‰ and -61 to -37‰, respectively (Table 4, Fig. 8). Overall, the quartz fluid inclusion waters have δD compositions lighter than the calcite fluid inclusion waters. As would be expected from this relationship, the δD values of the quartz/calcite mix samples fall in between the pure quartz and calcite samples.

Fluid-inclusion waters were extracted by thermal decrepitation for this study include water from primary and secondary fluid inclusions. Simmons (1986) selected samples of quartz, calcite, and sphalerite with high concentrations of primary inclusions for hydrogen-isotope analyses. His results are very similar to those of this study suggesting that the effects of secondary inclusions are minimal or the fluids trapped in both kinds of inclusions are very similar.

Fluid inclusion gas-analysis data

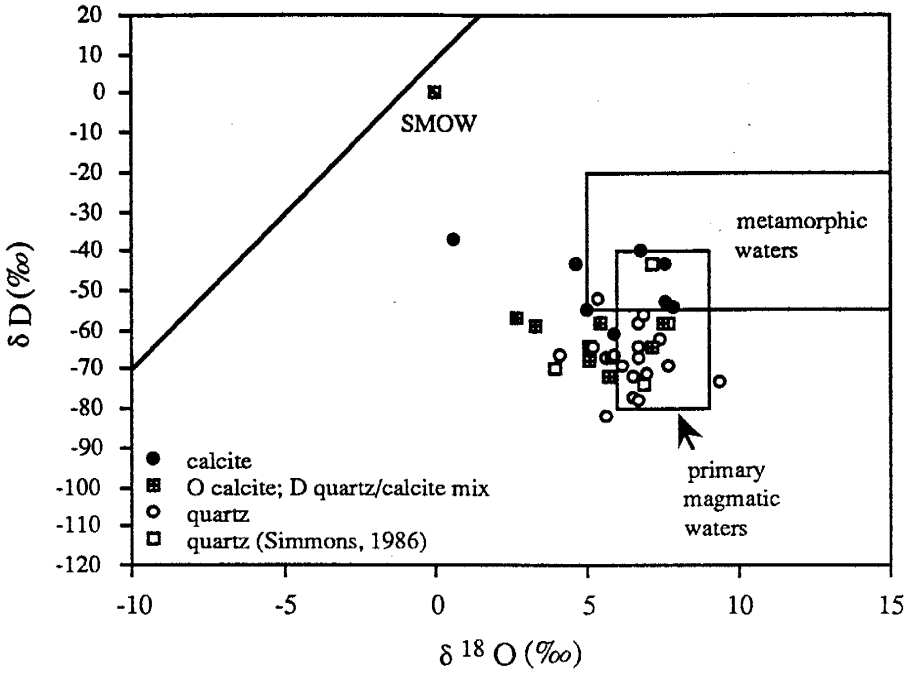

Figure 8. Oxygen and hydrogen-isotope composition of solutions compared to magmatic, metamorphic, and meteoric waters (Taylor, 1979). All values are relative to SMOW.

The concentration of gases from 16 quartz samples were calculated by the standard inverted matrix method using the peak intensities, the mass spectra and the probabilities of ionization (Norman and Sawkins, 1987). Water accounted for 96.7 to 99.9% of the volatiles liberated from the fluid inclusions. The predominant gases identified were H_2, CO_2, CH_4, N_2, H_2S, SO_2, NO, CO, and C_xH_n (combined organics) with lesser amounts of He, Ne, Ar, O_2, and NH_3 (Table 5). Data are recorded in mole percent and water is considered as a gaseous specie. The occurrence of high NO concentrations is the result of the cleaning process in which HNO_3 was used. N_2 values are also suspect.

During thermal decrepitiation, the gases may have reequilibrated resulting in the increase in CO_2 and H_2 at the expense of H_2O and CH_4 by the following reaction:

$$2H_2O + CH_4 => CO_2 + 4H_2$$

An unpublished, in house computer program (**GASFIX**) has been developed for this case by D.I. Norman to calculate gas concentrations more representative of the species present at the trapping temperature of the fluid inclusions based on thermodynamic data from Bowers *et al.* (1984) and Robie *et al.* (1979). The concentrations of CO_2, CH_4, H_2, CO, and H_2S, the oxygen fugacities, and sulfur fugacites were recalculated using **GASFIX** (Table 6).

Oxygen fugacities were calculated with using the temperatures listed in table 4, the gas data, and the following 5 equilibrium reactions:

(1) $H_2O = H_2 + {}^1/_2O_2$

(2) $CO_2 = C + O_2$

(3) $CO_2 + 2H_2 = CH_4 + O_2$

(4) $C + 2H_2O = CH_4 + O_2$

(5) $CO_2 + 2H_2O = CH_4 + 2O_2$

The results ranged from -39.8 to -42.5 log units (Table 6). The variation in log f_{O_2} values

TABLE 5. Gas Analysis data for quartz-hosted fluid-inclusions
(data are reported in mole percent)

Sample	H_2	CH_4	CO	N_2	NO	He
FR-88-6	2.18E-01	3.12E-02	3.79E-02	1.69E-01	5.54E-02	2.83E-04
FR-88-7	2.15E-02	1.23E-02	1.46E-02	4.59E-02	1.16E-02	4.82E-05
FR-88-10	1.38E-01	3.76E-01	-	1.55E-01	1.49E-01	8.35E-05
FR-88-11	1.17E-02	6.95E-02	-	1.51E-01	2.27E-02	7.46E-05
FR-88-14	3.57E-02	4.04E-02	3.83E-01	-	5.77E-02	1.71E-04
FR-88-20	5.16E-02	1.45E-01	-	1.77E-01	7.86E-02	8.10E-05
FR-88-21	8.79E-02	1.65E-01	1.48E-01	2.25E-01	1.76E-01	1.16E-04
FR-88-24	1.13E-02	7.11E-03	7.72E-03	1.38E-02	5.47E-03	4.04E-05
FR-88-25	2.89E-02	5.48E-02	3.25E-02	1.08E-01	4.74E-02	6.28E-05
FR-88-29	2.79E-02	8.99E-02	-	1.72E-01	3.52E-02	7.72E-05
FR-88-31	3.44E-01	1.63E-01	-	3.49E-01	1.71E-01	1.29E-04
FR-88-43	6.75E-02	2.57E-01	1.52E-02	2.20E-01	1.44E-01	1.52E-04
FR-88-47	3.98E-02	1.84E-01	6.56E-02	1.20E-01	6.56E-02	8.54E-05
FR-88-50	6.50E-02	2.48E-01	3.27E-01	5.38E-01	2.36E-01	2.07E-04
FR-88-54	1.05E-02	1.91E-02	1.14E-02	9.57E-02	4.92E-02	3.82E-05
FR-88-65	4.65E-02	4.19E-01	-	1.36E-01	1.16E-01	2.81E-05

Sample	Ne	Ar	O_2	NH_3	total H_2O
FR-88-6	1.07E-03	1.35E-03	-	-	9.91E+01
FR-88-7	2.39E-04	1.88E-04	-	-	9.96E+01
FR-88-10	6.77E-04	2.15E-04	-	-	9.85E+01
FR-88-11	5.51E-04	1.00E-03	1.26E-03	-	9.95E+01
FR-88-14	7.84E-04	8.21E-04	-	-	9.84E+01
FR-88-20	6.18E-04	2.90E-04	-	1.22E-03	9.90E+01
FR-88-21	5.12E-04	5.19E-04	-	-	9.85E+01
FR-88-24	5.60E-05	7.40E-05	-	-	9.99E+01
FR-88-25	3.86E-04	4.19E-04	-	-	9.94E+01
FR-88-29	5.28E-04	2.64E-04	2.72E-05	-	9.93E+01
FR-88-31	1.85E-03	1.33E-04	-	-	9.75E+01
FR-88-43	7.90E-04	9.84E-04	-	-	9.84E+01
FR-88-47	4.59E-04	6.26E-04	-	-	9.91E+01
FR-88-50	2.50E-03	1.22E-03	-	-	9.67E+01
FR-88-54	4.85E-04	2.91E-04	-	-	9.95E+01
FR-88-65	-	-	-	-	9.90E+01

TABLE 5. Continued

Sample	CO_2	SO_2	H_2S	CS_2	C_xH_n
FR-88-6	2.84E-01	3.67E-03	5.96E-03	9.86E-05	8.41E-02
FR-88-7	2.80E-01	9.39E-05	6.47E-04	2.14E-06	3.63E-02
FR-88-10	5.60E-01	2.55E-04	2.09E-02	4.15E-05	1.51E-01
FR-88-11	2.54E-01	9.02E-05	5.89E-04	2.03E-06	3.36E-02
FR-88-14	7.58E-01	1.45E-01	9.68E-04	7.73E-04	2.19E-01
FR-88-20	4.32E-01	3.57E-02	9.38E-05	1.62E-04	8.10E-02
FR-88-21	4.75E-01	1.25E-02	1.41E-02	2.82E-04	1.67E-01
FR-88-24	4.97E-02	2.07E-05	9.03E-05	2.34E-06	1.05E-02
FR-88-25	3.06E-01	4.28E-04	6.09E-05	9.08E-06	3.89E-02
FR-88-29	3.20E-01	6.78E-03	5.88E-05	4.52E-05	8.61E-02
FR-88-31	1.15E+00	1.41E-01	9.63E-02	5.74E-04	1.16E-01
FR-88-43	7.51E-01	5.63E-03	1.22E-03	1.22E-04	1.28E-01
FR-88-47	3.61E-01	8.28E-03	9.83E-05	3.29E-05	6.46E-02
FR-88-50	1.59E+00	8.73E-02	7.48E-05	5.73E-04	2.46E-01
FR-88-54	2.22E-01	7.63E-03	1.24E-05	5.27E-05	4.45E-02
FR-88-65	1.86E-01	5.66E-03	1.76E-02	1.74E-04	4.41E-02

TABLE 6. Gas data recalculated using **GASFIX**
(data are reported in mole percent)

Sample	H_2	CO	CH_4	CO_2	H_2S
FR-88-6	1.03E-04	3.79E-02	8.57E-02	2.30E-01	5.96E-03
FR-88-7	7.20E-05	1.46E-02	1.77E-02	2.75E-01	6.47E-04
FR-88-10	1.03E-04	-	4.10E-01	5.26E-01	2.09E-02
FR-88-11	8.40E-05	-	7.25E-02	2.51E-01	5.89E-04
FR-88-14	4.79E-05	3.83E-01	4.94E-02	7.49E-01	9.68E-04
FR-88-20	9.18E-05	-	1.58E-01	4.19E-01	9.38E-05
FR-88-21	9.95E-05	1.48E-01	1.87E-01	4.53E-01	1.41E-02
FR-88-24	1.28E-04	7.72E-03	9.90E-03	4.69E-02	9.03E-05
FR-88-25	1.28E-04	3.25E-02	6.20E-02	2.99E-01	6.09E-05
FR-88-29	1.80E-04	-	9.68E-02	3.13E-01	5.88E-05
FR-88-31	6.16E-05	-	2.49E-01	1.06E+00	9.63E-02
FR-88-43	1.48E-04	1.52E-02	2.74E-01	7.34E-01	1.22E-03
FR-88-47	9.99E-05	6.56E-02	1.94E-01	3.51E-01	9.38E-05
FR-88-50	1.32E-04	3.27E-01	2.64E-01	1.57E+00	7.48E-05
FR-88-54	1.56E-04	1.14E-02	2.17E-02	2.19E-01	1.24E-05
FR-88-65	2.00E-04	-	4.31E-01	1.74E-01	1.76E-02

for a single gas analysis is a maximum of 2.4 log units with an average of 1.5 log units. Sulfur fugacities are calculated using oxygen fugacities obtained from equation 5 with the following equation:

$$2H_2S + O_2 = S_2 + 2H_2O$$

Values range from -10.5 to -17.9 log units (Table 7).

Gases are from primary and secondary inclusions. Hydrogen-isotope data suggests that the contribution of secondary inclusions are minimal or the inclusion trapped fluids are similar in their overall nature.

Gas-analysis data relationships

The depth, approximate temperature, total mole percent H_2O, and the $\log_{10}$ of the oxygen fugacity and principal gas components were analyzed by factor analysis. The unrotated factor matrix is presented in Table 8. The results indicate two factors. The first factor consists of strong covariance between CO_2, CH_4, N_2, SO_2, CO, Ne, Ar, He, CS_2, C_xH_n, total mole percent H_2O, and to a much weaker extent H_2S and depth. The second factor consists of H_2, temperature, depth, and log f_{O_2} which have a strong negative correlation to H_2S, which is closely related to sulfur fugacity, and to a much weaker extent He.

Data intra-relationships

$^{87}Sr/^{86}Sr$, stable isotopes, gas concentrations, f_{S_2}, and f_{O_2} were compared to one another in addition to stage of mineralization, approximate temperature, depth, and host rock. Depth and host rock information for sample locations are listed in Appendix D. Calcite and quartz derived data were examined separately. Gas concentrations were only analyzed from quartz hosted fluid inclusions. Hence, no relationships were evident

TABLE 7. Oxygen and sulfur fugacities

Sample	eq. 1 log fO_2	eq. 2 log fO_2	eq. 3 log fO_2	eq. 4 log fO_2	eq. 5 log fO_2	log fS_2
FR-88-6	-41.7	-41.1	-41.5	-42.1	-41.6	-12.9
FR-88-7	-41.3	-41.0	-41.0	-41.3	-41.1	-14.5
FR-88-10	-42.6	-41.1	-42.0	-43.5	-42.3	-12.1
FR-88-11	-42.4	-41.4	-41.8	-42.7	-42.1	-15.0
FR-88-14	-41.9	-41.1	-41.8	-42.5	-41.8	-14.2
FR-88-20	-42.2	-41.0	-41.7	-42.8	-41.9	-16.6
FR-88-21	-42.2	-41.0	-41.7	-42.9	-41.9	-12.3
FR-88-24	-41.0	-41.2	-40.6	-40.4	-40.8	-16.4
FR-88-25	-41.0	-40.4	-40.6	-41.2	-40.8	-16.7
FR-88-29	-40.6	-39.9	-40.1	-40.8	-40.3	-16.8
FR-88-31	-42.6	-41.3	-42.4	-43.7	-42.5	-10.5
FR-88-43	-41.1	-40.0	-40.7	-41.8	-40.9	-14.3
FR-88-47	-42.1	-41.2	-41.9	-42.8	-42.0	-16.7
FR-88-50	-40.7	-39.5	-40.3	-41.5	-40.5	-16.5
FR-88-54	-40.1	-39.8	-39.6	-39.8	-39.8	-17.9
FR-88-65	-42.1	-40.9	-41.4	-42.6	-41.8	-12.4
average	-41.6	-40.7	-41.2	-42.0	-41.4	

TABLE 8. Unrotated factor matrix of gas and related data

	Factor 1	Factor 2
total H_2O	-0.89	-0.17
log (H_2)	0.15	0.84
log (CO_2)	0.90	0.10
log (CH_4)	0.92	-0.13
log (H_2S)	0.30	-0.80
log (SO_2)	0.93	0.20
log (N_2)	0.98	0.07
log (CO)	0.82	-0.14
log (He)	0.83	-0.34
log (Ar)	0.92	-0.12
log (Ne)	0.94	0.09
log (CS_2)	0.93	0.12
log (C_xH_n)	0.98	-0.07
T (°C)	-0.02	0.84
Depth	0.43	0.66
log fO_2	-0.18	0.89

between the quartz and calcite data and the stage of mineralization or the wall rocks, except for the $^{87}Sr/^{86}Sr$ values of stage IV calcites which are more consistent than any other stage (Fig. 9); values of 4 samples fall in the narrow range of 0.7086 to 0.7089. For quartz derived data, $\delta^{18}O_{H_2O}$ correlate positively with estimated temperatures (Fig. 10) and log f_{S_2} and H_2S, which are closely related, correlate negatively with δD (Figs. 11). For calcite derived data, $^{87}Sr/^{86}Sr$ values negatively correlate with $\delta^{13}C$ and to a lesser extent positively with $\delta^{18}O_{H_2O}$ (Fig. 12).

DISCUSSION

Physicochemical composition of the fluids

The range of oxygen fugacities is narrow for those calculated from gas data for each sample and from different equilibrium equations including two that assume equilibrium with C. These values suggest that the oxygen fugacity of the hydrothermal fluids was buffered with respect to C by the C-rich wall rocks. This resulted in hydrothermal fluids with equilibrium concentrations of CO_2 and CH_4 that are, in part, related to the oxygen fugacity and restricted it to a narrow range of values. Sulfur fugacitites calculated have a range of values (log f_{S_2} = -17.9 to -10.5) similar to those proposed by Gemmell (1986) based on sulfide, sulfosalt, and gangue mineral assemblages (log f_{S_2} = -17 to -11). Oxygen and sulfur fugacities are inversely related and both covary with temperature. The variation of the sulfur and oxygen fugacities during mineral deposition are presented in Fig. 13. The fugacities are recalculated for 250°C. The data plot within the pyrite, pyrrhotite, chlorite, and magnetite fields. Pyrite, pyrrhotite, and chlorite are present, however, magnetite is absent from the mineralogy of the Santo Niño vein (Gemmell, 1986). The magnetite field might be completely pre-empted by chlorite (Barton *et al.*, 1977) which can explain the absence of magnetite. Hence, the data suggest that Fe-bearing mineral assemblages were controlled by variable sulfur fugacities.

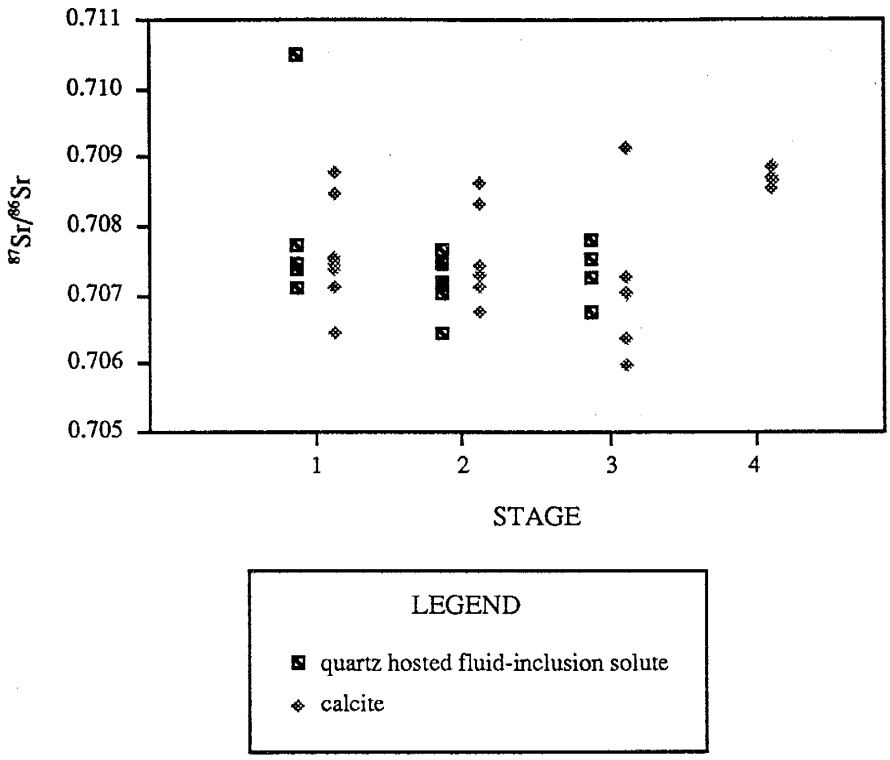

Figure 9. Distribution of Sr-isotope composition of vein calcite with respect to stage.

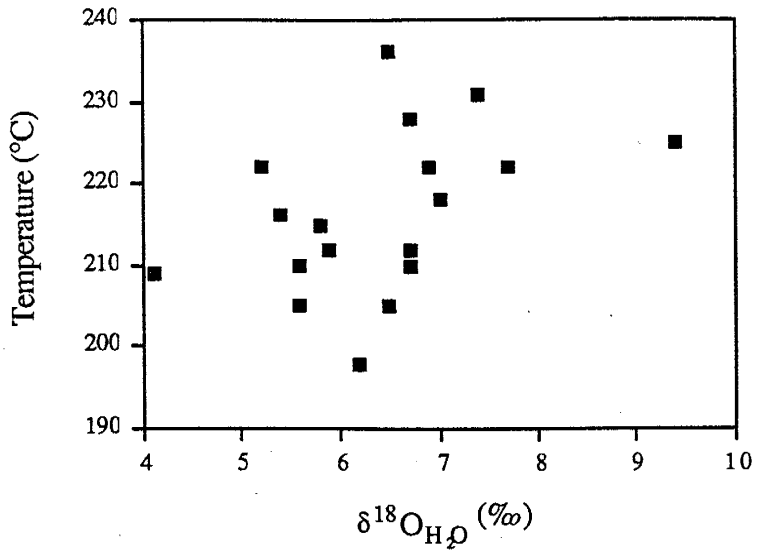

Figure 10. Temperature-$\delta^{18}O_{H_2O}$ plot for quartz samples. Oxygen-isotope values are relative to SMOW.

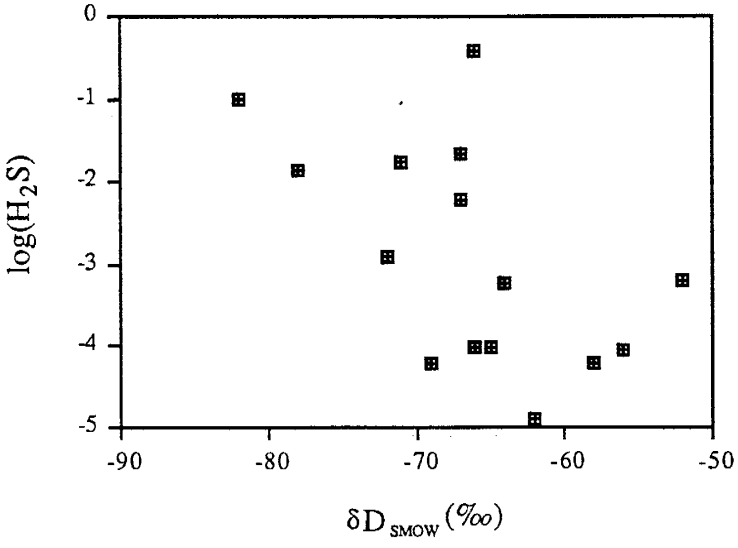

Figure 11. Log (H_2S)-δD plot for fluid inclusion gases and waters

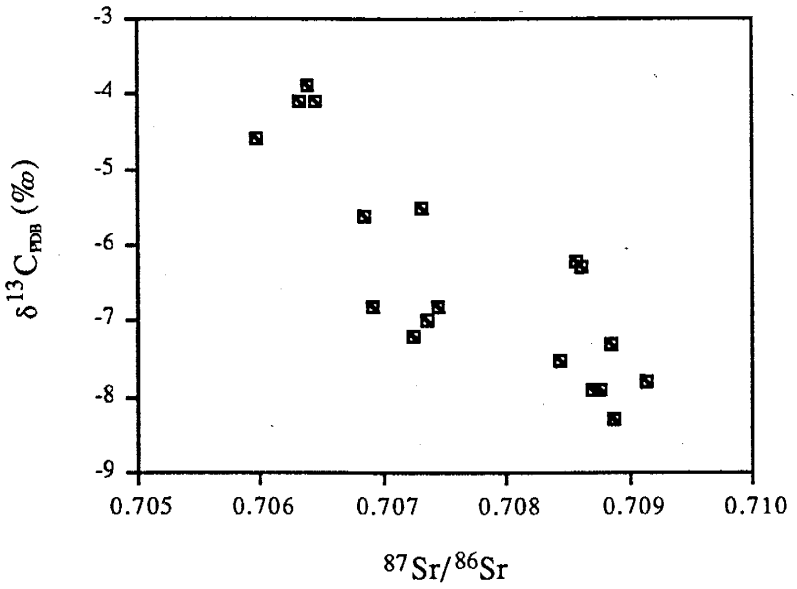

Figure 12. $\delta^{13}C$-$^{87}Sr/^{86}Sr$ plot for calcite samples.

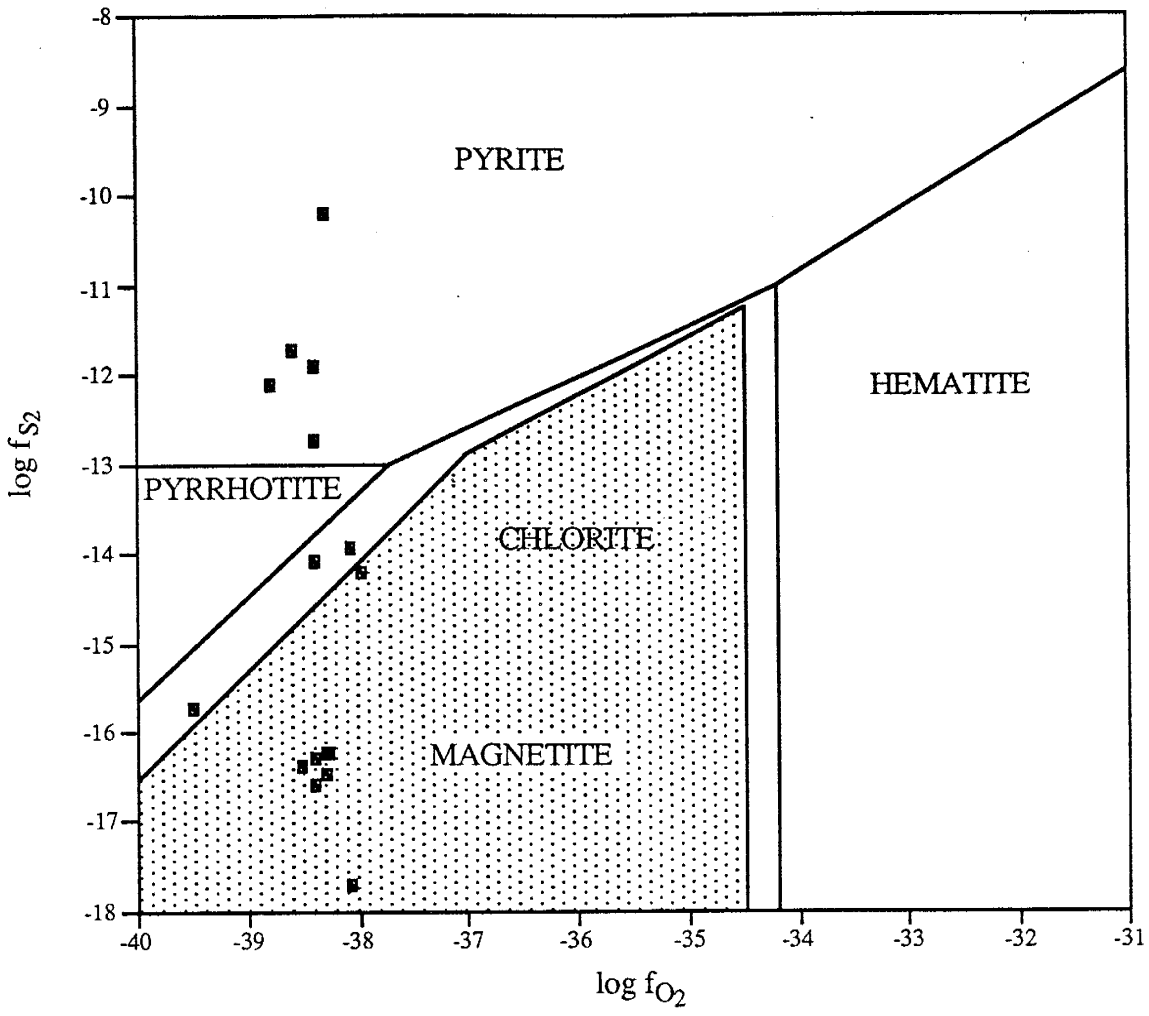

Figure 13. Log f_{S_2} vs. log f_{O_2} diagram at 250°C showing stability fields of minerals pertinent to the interpretation of the Santo Niño vein. The shaded magnetite field is completely preempted by chlorite. Quartz is ubiquitous. Diagram after Barton *et al.* (1977).

Effects of boiling

The first factor in Table 7 indicates that most gases are strongly correlated. Since, boiling can cause elevated amounts of gas to be trapped in vapor-fluid inclusions, this relationship may represent the factionation of gases into a vapor phase during boiling (Norman and Sawkins, 1987). Alternatively, this factor may represent the addition of a gas-rich fluid to the hydrothermal system. In light of fluid inclusion evidence for boiling throughout the Santo Niño vein, the former scenario is favored here.

The second factor described in Table 7 is more difficult to interpret. Microthermetric fluid-inclusion studies indicate that areas of the vein with lower temperatures also have higher salinities (Querol *et al.*, 1989). In addition, these regions correspond to higher concentrations of H_2S in the fluid-inclusion gases in areas of adequate sample density. This suggests that salinity also inversely varies in this factor like H_2S. The association of lower temperatures and higher salinities suggests that the second factor may represent the liquid phase of a boiling system. For open system boiling, oxygen fugacity increases as the ratios of CO_2:CH_4 and SO_2:H_2S increase because CH_4 and H_2S partition into the vapor phase at a greater rate than CO_2 and SO_2, respectively (Drummond and Ohmoto, 1979). In addition, the salinity will increase and the temperature should decrease as liquid is lost to the vapor phase (Buchanan, 1981). However, this factor indicates an increase in salinity and H_2S with a decrease in temperature and oxygen fugacity suggesting that boiling is not the only controlling mechanism. At least two fluids have been inferred from the fluid inclusion data from Chico (1986) and Simmons (1986), one of higher salinity and one of lower salinity according to Ruvalcaba-Ruiz and Thompson (1988). In addition, the data suggest intense boiling occurs with sharp salinity increases. Gemmell (1988) proposes that multiple fissure openings provided conduits for the ore-bearing fluids. Therefore, this factor may represent fissure openings that allow a higher salinity, H_2S-rich fluid to enter the system. In addition, pressure release caused by the fissure openings results in intense boiling of the fluid. A combination of boiling and

mixing with the low salinity fluid which may have a high oxygen fugacity and a low sulfur fugacity would produce the observed fugacities. Whether the low temperatures associated with high salinity fluid are a characteristic of the
fluid or the result of the fluid being cooled cannot be determined.

As hydrothermal fluids boil over time, isotopic fractionation occurs with phase separation that may affect both $\delta^{18}O_{H_2O}$ and δD values. During boiling, a cross-over point exists at about 220°C for hydrogen isotopes (Bottinga and Craig, 1968). Above this temperature, HDO partitions into the vapor phase; below it, HDO partitions into the liquid phase. The approximate deposition temperature of the Santo Niño vein mineralization is very close to the cross-over temperature. Hence, the effect of boiling on the hydrogen-isotope values is minimal. Similarly, the range of $\delta^{18}O_{H_2O}$ values measured can only be the result of extreme boiling. The approximate amount of water that needs to be vaporized to produce the observed change in quartz derived $\delta^{18}O_{H_2O}$ values, 4.1 to 9.4‰, and can be calculated using Raleigh's Law and assuming constant temperature (Kamilli and Ohmoto, 1977):

$$\delta_l - \delta_o = 1000\ (f^{(\alpha-1)} - 1)$$

for which
- δ_l = $\delta^{18}O_{H_2O}$ after the vaporization of a certain amount of liquid
- δ_o = $\delta^{18}O_{H_2O}$ at the start of boiling
- f = the fraction of liquid remaining
- α = the isotopic fractionation factor between water vapor and liquid water

Samples FR-88-7 and FR-88-65 are both from stage III and have similar temperatures. The $\delta^{18}O_{H_2O}$ values are 5.4‰ and 7.0‰, respectively, for these samples. Using the fractionation factor at 217°C of 0.99794 calculated using an equation from Bottinga and Craig (1968) and the equation of Kamilli and Ohmoto, 53% of the liquid would have to be vaporized to produce the $\delta^{18}O_{H_2O}$ values observed. The enthalpy required for 53% of the

fluid to be boiled away is approximately 1970 J/g liquid and corresponds to a temperature of 373°C (Henley *et al.*, 1984). Fluid temperatures this high have been reported for the deep chimneys, mantos, and veins, but there was no indication of boiling from fluid inclusion studies (Kreczmer, 1977; MacDonald, 1978; Chico, 1986; Ruvalcaba-Ruiz and Thompson, 1988). Therefore, any variations in the $\delta^{18}O_{H_2O}$ values caused by boiling are likely to be very small.

Effects of CO_2 on freezing point measurements of fluid inclusions

The CO_2 concentrations measured for fluid inclusion volatiles ranges from 0.05 to 1.57 mole percent. According to Hedenquist and Henley (1985), these concentrations can cause freezing point depression in epithermal fluid inclusions from -0.1 to -1.7°C, respectively. The presence of dissolved CO_2 may explain some of the widely varying melting temperatures measured for adjacent inclusions by Simmons (1986).

Fluid and wall-rock interaction

Vein calcite $^{87}Sr/^{86}Sr$ values vary inversely with $\delta^{13}C$ and to a lesser extent $\delta^{18}O_{H_2O}$ (Fig. 10). This relationship may represent the mixing of two fluids. The quartz monzonite intrusion could have provided the less radiogenic fluid and the magmatic systems responsible for the younger volcanic units could have contributed the more radiogenic fluid if the $\delta^{13}C$ values of the two fluids are approximately -4‰ and -8‰, respectively.

Since hydrogen is in small concentrations in wall rocks, the absence of a correlation with δD suggests that the $^{87}Sr/^{86}Sr$, $\delta^{13}C$, and to a lesser extent $\delta^{18}O_{H_2O}$ composition of the mineralizing fluids is controlled by water-rock interaction, and by not isotopically distinct fluids. However, water-rock interaction during mineralization was very limited after stage I (Dr. F. Querol pers. com.), indicating that exchange occured elsewhere and was transported to the sit of mineralization later. The Chilitos Formation andesites and the lutite shales could have provided Sr required to produce the observed values. Syndepositional

alteration of the andesite by seawater may have contributed significant carbon to the andesites resulting in an overall carbon isotope composition of approximately -4%. The Middle Cretaceous limestones in the area also could have provided similar $\delta^{13}C$ values. However, the $^{87}Sr/^{86}Sr$ composition of Middle Cretaceous marine carbonates are too radiogenic to account for the observed values (Faure, 1986). Therefore, the Fortuna and Cerro Gordo limestones are unlikely source of fluid components. The black shales of the lutite could have provided light carbon of organic origin. Ultimately, the source of the Sr in the vein mineralization cannot be unequivocally determined from the data obtained for the country and intrusive rocks because of the wide variety of $^{87}Sr/^{86}Sr$ values and insufficient carbon isotope data.

In the Santo Niño vein, quartz gangue is more closely associated with the ore mineralization than is calcite. In addition, most quartz-hosted fluid inclusion samples fall into a smaller range of $^{87}Sr/^{86}Sr$ values (0.70764 to 0.7078) than the calcite $^{87}Sr/^{86}Sr$ values. This suggests that the two minerals may have been precipitated from either a fluid that has taken different paths to the vein and modified differently, two different fluids, or fluids that have undergone varying degrees of mixing. Stable isotope data discussed in the following section suggests that two fluids are responsible for the mineralization. Since all analyses are from bulk samples the subtleties of fluid interaction cannot be determined.

Origin of the solutions

The stable isotope data suggest the contributions of magmatic and exchanged meteoric waters (Taylor, 1974; Campbell *et al.*, 1984) (Fig. 14). The contribution of a basinal brine is discounted by Simmons *et al.* (1988). The wide range of $\delta^{18}O_{H_2O}$ values with heavy δD values around -40‰ does not suggest simple mixing of two distinct fluids. These values may be the result of two mechanisms: (1) the meteoric fluid has undergone varying degrees of isotopic exchange with the wall rocks; and/or (2) waters of

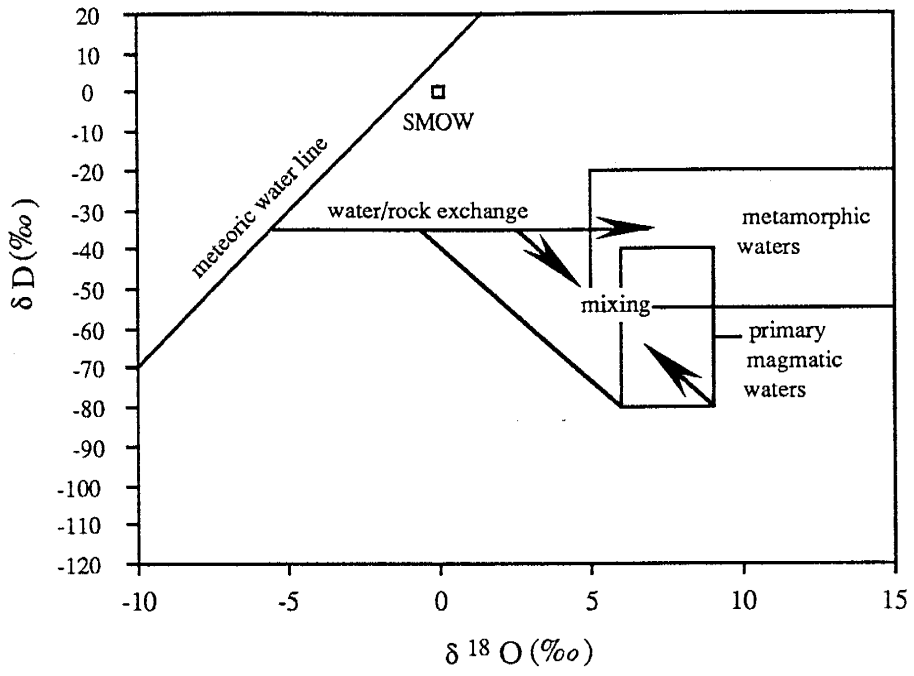

Figure 14. Schematic diagram of possible fluid sources and processes; magmatic, metamorphic, and meteoric water compositions from Taylor (1974).

predominantly meteoric composition from secondary inclusions modified the δD values of the water significantly, but the $\delta^{18}O$ values of the quartz and calcite were effected minimally. However, the metamorphic-like $\delta^{18}O_{H_2O}$ values reported for stage IV calcites in Simmons (1986) and Simmons *et al.* (1988) could not be reproduced in this study. Therefore, it is the opinion of the author that no significant change occured in the stable-isotopic composition (i.e. source) of the calcite depositing fluids between the first stages and stage IV.

Previous geochemical studies of the Fresnillo ore bodies favor a magmatic origin for the ore-bearing solutions (MacDonald *et al,* 1986; Simmons, 1986). The relationship of light δD values with higher sulfur fugacities and higher concentrations of H_2S suggest that these components, which are also related to regions of higher fluid inclusion salinities, are added to the system by a magmatic fluid. However, one δD analysis of water from relatively high salinity sphalerite sample gave a value of -30‰ which is out of the accepted range for magmatic fluids.

In general, the quartz fluid inclusion waters have lighter δD values than the calcite fluid inclusion waters. The δD values of the quartz/calcite mix samples fall in between the pure quartz and calcite samples. This relationship suggests that the calcite depositing fluids may be more meteoric in composition and the quartz depositing fluids may be more magmatic in composition. However, both low and relatively high salinities have been reported for both quartz and calcite fluid inclusions (Simmons *et al.*, 1988). The variety of salinities may be the result of mixing and/or that two magmatic fluids, one dilute and one saline, in addition to a meteoric fluid may have been present. If two magmatic fluids are present, they may have the same or different sources. Both scenarios would be fairly similar. Each stage would represents a pulse of high salinity, H_2S-rich fluid which either became more diluted as it evolved or by mixing with the lower salinity fluid. In both cases some dilution could also be attributed to mixing with the meteoric component.

CONCLUSIONS

(1) Oxygen fugacities of ore fluids are buffered by the carbon-rich wall rocks. The sulfur fugacities vary widely. The precipitation of Fe-bearing mineral assemblages was controlled by variable sulfur fugacities.

(2) In the Santo Niño vein, regions of lower fluid inclusion Th and higher salinities coincide with the locations of inclusions with higher H_2S concentrations.

(3) Factor analysis indicates the partitioning of gases into a vapor phase during boiling. A second factor suggests the addition of of a higher salinity, H_2S-rich fluid to the mineralizing system. A combination of boiling and mixing with a lower salinity fluid produced the observed sulfur and oxygen fugacities (f_{S_2} = -17.9 to -10.5; f_{O_2} = -42.5 to -39.8).

(4) The presence of dissolved CO_2 in fluid inclusion accounts for some of the widely varying melting temperatures measured for adjacent inclusions by Simmons (1986).

(5) The $^{87}Sr/^{86}Sr$, $\delta^{18}C$, and to a lesser extent $\delta^{18}O_{H_2O}$ composition of vein calcites are controlled by interaction between the hydrothermal fluids and the host rocks. The sources of these components cannot be identified unequivocally. However, the most likely sources are the andesites of the Chilitos Formation and the sediments of the lutite and upper greywacke units.

(6) Oxygen and hydrogen isotope data suggest the mineralizing fluids were a combination of an exchanged meteroric and a magmatic.

(7) Most quartz fluid inclusion solute $^{87}Sr/^{86}Sr$ values have a smaller range than the calcite values and quartz derived δD values tend to be lighter than calcite derived values. These relationships suggest that the mineral-depositing fluids had Sr from different sources and that the magmatic fluid was quartz-saturated and the exchanged meteoric fluid was calcite-saturated.

REFERENCES

Albinson, T.F., 1988, Geologic reconstruction of paleosurfaces in the Sombrerete, Colorada, and Fresnillo districts, Zacatecas state, Mexico: Econ. Geol., vol. 83, p. 1647-1667.

Bargalló, M., 1955, La mineria y la meralurgia en la América española durante la época colonial: Mexico, D.F., Fondo de Culrura Económica, 442 p.

Benton, L.D., 1987, Trace element and strontium isotope composition of the calcites of the Santo Niño vein, Fresnillo district, Zacatecas, Mexico: Unpubl. B.A. thesis, Dartmouth College, 39 p.

Borthwick, J., and Harmon, R.S., 1982, A note regarding ClF_3 as an alternative to BrF_5 for oxygen isotope analysis: Geoch. et Cosmochim. Acta, vol. 46, p. 1665-1668.

Bottinga, Y., and Craig, H., 1968, High temperature liquid-vapor fractionation factors for H_2O-HDO-H_2O^{18}: Am. Geoph. Union Trans., vol. 49, p. 356-357.

Bottrell, S.H., Yardley, B., and Buckley, F., 1988, A modified crush-leach method for the analysis of fluid inclusion electrolytes: Bull. Minéral., vol. 111, p. 279-290.

Bowers, T.S., Jackson, K.J., and Helgeson, H.C., 1984, Equilibrium Activity Diagrams: New York, Springer-Verlag, 397 p.

Buchanan, L.J., 1981, Precious metal deposits associated with volcanic environments in the southwest, *in* Dickinson, W.R., and Payne, W.D., eds., Relationships of Tectonics to Ore Deposits in the Southern Cordillera: Tuscon, Arizona Geological Society Digest, vol. XIV, p. 237-262.

Campa, M.F., and Coney, P.J., 1983, Tectono-stratigraphic terranes and mineral resource distribution in Mexico: Can. Jour. Earth Sci., v. 20, p. 1040-1051.

Campa, M.F., and Coney, P.J., 1985, The Mexican thrust belt:*in* Howell, D.G., ed.,Tectonostratigraphic Terranes of the Circum-Pacific Region: Circ. Pac. Counc. Energ. Min. Res., No. 1, p. 299-312.

Campbell, A., Rye, D., and Petersen, U., 1984, A hydrogen and oxygen isotope study of the San Cristobal mine, Peru: Implications of the role of water to rock ratio for the genesis of wolframite deposits: Econ. Geol., vol. 79, p. 1818-1832.

Clark, K.F., Foster, C.T., and Damon, P.E., 1982, Cenozoic mineral deposits and subduction-related magmatic arcs in Mexico: Geol. Soc. Am. Bull., vol. 93, p. 533-544.

Clayton, R.N., O'Neil, J.R., and Mayeda, T., 1972, Oxygen isotope exchange between quartz and water: J. Geophys. Rev., vol. 77, p. 3057-3067.

Chico, E., 1986, Mineralogy, paragenesis, and fluid inclusion studies in three veins of the Fresnillo, Mining District, Zacatecas, Mexico: Unpubl. M.S. thesis, Dartmouth College, 114 p.

Coleman, M.L., Shepherd, T.J., Durham, J.J., Rouse, J.E., and Moore, G.R., 1982, Reduction of water with zinc reagent for hydrogen isotope analysis: Anal. Chem., vol. 54, p. 993-995.

Davila Alcocer, V.M., 1981, Radiolarians del Cretácico Inferior de la Formación Plateros, distrito minero de Fresnillo, Zacatecas: Nota Pública en la Revista Del Instituto De Geología, vol. 5, No. 1, p. 119-120.

De Cserna, Z., 1976, Geology of the Fresnillo area, Zacatecas, Mexico: Geol. Soc. Am. Bull., vol. 87, p. 1191-1199.

Drummond, S.E., and Ohmoto, H., 1979, Effects of boiling on mineral solubilities in hydrothermal solutions: Geol. Soc. Am. Abs., 92nd Ann. Mtg., San Diego, p. 416.

Farmer, G.L., and DePaolo, D.J., 1987, Nd and Sr isotope study of hydrothermally altered granite at San Manuel, Arizona: Implications for element migration paths during the formation of porphyry copper ore deposits: Econ. Geol., vol. 82, p. 1142-1151.

Faure, G., 1986, Principles of Isotope Geology: New York, John Wiley and Sons, 589 p.

García, E., Querol, F., and Lowther, G.K., 1989, Geología del distrito de Fresnillo, Zacatecas: Geol. Soc. America, DNAG series, vol. P-3.

Gemmell, J.B., 1986, The Santo Niño Ag-Pb-Zn vein, Fresnillo district, Mexico: Geology, sulphide, and sulphosalt mineralogy, and geochemistry: Unpubl. Ph.D. thesis, Dartmouth College, 244 p.

Gemmell, J.B., Simmons, S.F., and Zantop, H., 1988, The Santon Niño silver-lead-zinc vein, Fresnillo district, Zacatecas, Mexico: Part I. Structure, vein stratigraphy, and mineralogy: Econ. Geol., vol. 83, p. 1597-1818.

Gemmell, J.B., Zantop, H., and Birnie, R.W., 1989, Silver sulfosalts of the Santo Niño vein, Fresnillo district, Zacatecas, Mexico: Can. Min., vol. 27, p. 401-418.

Hedenquist, J.W., and Henley, R.W., 1985, The importance of CO_2 on freezing point measurements of fluid inclusions: Evidence from active geothermal systems and implications for epithermal ore deposits: Econ. Geol., vol. 80, p. 1379-1406.

Henley, R.W., Truesdell, A.H., Barton, Jr., P.B., and Whitney, A.J., 1984, Robertson, J.M., ed., Fluid-Mineral Equilibria in Hydrothermal Systems: El Paso, Texas, Society of Economic Geologists, 267 p.

Kamilli, R.J., and Ohmoto, H., 1977, Paragenesis, zoning, fluid inclusion, and isotopic studies of the Finlandia vein, Colqui district, central Peru: Econ. Geol., vol. 72, p. 950-982.

Koch, G.S., Jr., and Link, R.F., 1967, Geometry of metal distribution in five veins of the Fresnillo mine, Zacatecas, Mexico: U.S. Bur. Mines Rept. Inv. 6919, 64 p.

Kreczmer, M.J., 1977, The geology and geochemistry of the Fortuna mineralization, Fresnillo, Zacatecas, Mexico: Unpubl. M.Sc. thesis, University of Toronto, 155 p.

Lang, B., Steinitz, G., Sawkins, F.J., and Simmons, S.F., 1988, K-Ar age studies in the Fresnillo silver district, Zacatecas, Mexico: Econ. Geol., vol. 83, p. 1642-1646.

Lowther, G.K., 1981, Brief notes in history, past and present production and reserves of the Proaño mine, Fresnillo: Unpubl. Fresnillo Company Report.

Lucio, J.A., 1990, A Pb and Sr study of the Fresnillo Mining District, Zacatecas, Mexico: Unpubl. M.Sc. thesis, Dartmouth College, 89 p.

MacDonald, J.A., 1978, The geology and geochemistry of the Cueva Santa Branch Ag-Pb-Zn manto ore body, Fresnillo mine, Zacatecas, Mexico: unpubl. M.Sc. thesis, University of Toronto, 129 p.

MacDonald, J.A., Kreczmer, M.J., and Kesler, S.E., 1986, Vein, manto, and chimney mineralization at the Fresnillo silver-lead-zinc mine, Mexico: Can. Jour. Earth Sci., vol. 23, p. 1603-1614.

McCrea, J.M., 1950, The isotopic chemistry of carbonates and a paleotemperature scale: J. Chem. Phys., vol. 18, p. 849.

Norman, D.I., 1978, Analysis of Rb, Sr, and Sr isotopes in fluid inclusion waters: Inst. Mining Metallurgy Trans., sec. B., vol. 87, p. 34-35.

Norman, D.I., and Landis, G.P., 1983, Source of mineralizing components in hydrothermal ore fluids as evidenced by $^{87}Sr/^{86}Sr$ and stable isotope data from the Pasto Bueno deposit, Peru: Econ. Geol., vol 78, p. 451-465.

Norman, D.I., and Sawkins, F.J., 1987, Analysis of volatiles in fluid inclusions by mass spectrometry: Chem. Geol., vol. 61, p. 1-10.

O'Neil, J.R., Clayton, R.N., and Mayeda, T., 1969, Oxygen isotope fractionation in divalent metal carbonates: J. Chem. Phys., vol. 51, p. 5547-5558.

Querol, F., 1980, Estudio petrológico de la Formación Chilitos y del conglomerado de la Formación Fresnillo, Fresnillo, Zacatecas: Unpubl. Fresnillo Company Report, 8 p.

Querol, F., Yza, R., Palacios, H., and Herrera, H., 1989, Geologia y microthemometria de las vetas del area San Luis del Distrito Fresnillo, Zacatecas.

Robie, R.A., Hemingway, B.S., and Fisher, J.R., 1979, Thermodynamic Properties of Minerals and Related Substances at 298.15 K and 1 Bar (10^5 Pascals) Pressure and at Higher Temperatures, Washington, D.C., United States Government Printing Office, 456 p.

Roedder, E., 1958, Technique for the extraction and partial chemical analysis of fluid-filled inclusions from minerals: Econ. Geol., vol. 53, p. 235-269.

Roedder, E., 1963, Studies of fluid inclusions III: Extraction and quantitative analysis of fluid inclusions in the milligram range: Econ. Geol., vol. 58, p. 353-374.

Ruvalcaba-Ruiz, D.C. and Thompson, T.B., 1988,Ore deposits at the Fresnillo mine, Zacatecas, Mexico: Econ. Geol., vol. 83, p. 1583-1596.

Shepard, T.M., Rankin, A.H., and Alderton, D.H.M., 1985, A Practical Guide to Fluid Inclusion Studies: London, Blackie and Sons Limited, 239 p.

Simmons, S.F., 1985, Geology and paleohydrothermal activity of the Fresnillo district, Zacatecas, Mexico: Unpubl. Fresnillo Company Report, 16 p.

Simmons, S.F., 1986, Physico-chemical nature of the mineralizing solutions for the St. Niño vein: results of fluid inclusion, deuterium, oxygen, and helium studies in the Fresnillo district, Zacatecas, Mexico: Unpub. Ph.D. thesis University of Minnesota at Minneapolis, 191 p.

Simmons, S.F., Gemmell, J.B., and Sawkins, F.J., 1988, The Santo Niño Silver-Lead-Zinc Vein, Fresnillo District, Zacatecas, Mexico: Part II. Physical and chemical nature of ore-forming solutions: Econ. Geol., vol. 83, p. 1619-1641.

Stone, J.B., and McCarthy, J.C., 1948, Mineral and metal variations in the veins of Fresnillo, Zacatecas, Mexico: Am. Inst. Mining Metall. Engineers Trans, vol. 148, p. 91-106.

Taylor, H.P., 1974, The application of oxygen and hydrogen isotope studies to problems of hydrothermal alteration and ore deposition: Econ. Geol., vol. 69, p.843-883.

Taylor, H.P., 1979, Oxygen and hydrogen isotope relationships in hydrothermal mineral deposits: *in* Barnes, H.L.,ed., Geochemistry of Hydrothermal Ore Deposits: New York, J. Wiley and Sons, p. 236-272.

Taylor, H.P., and Epstein, S., 1962, Relationship between $^{18}O/^{16}O$ ratios in coexisting minerals of igneous and metamorphic rocks, Part I: Principles and experimental results: Bull. Geol. Soc. Am., vol. 73, p. 461-480.

Vallejo, A., 1983, Informe de resultados obtenidos a la fecha del estudio geológico superficial en el proyecto región Fresnillo, Zacatecas: Unpubl. Fresnillo Company report, 20 p.

Ward, D., 1990, Digestion and separation procedure for routine Rb-Sr analysis of silicates: Unpubl. lab procedures, University of New Mexico at Albuquerque, 6 p.

Weast, R.C., and Grasselli, J.G., 1990, CRC Handbook of Data on Organic Compounds: Boca Raton, FL, CRC Press, vol. 5, 3538 p. and vol. 4, 2727 p.

Appendix A: Strontium Isotope Analytical Methods for Fluid Inclusion Solute

The vein quartz and sulfide samples from which fluid inclusion solute was analyzed for strontium isotopes were prepared by the following process adapted from Roedder (1958, 1963), Norman (1978) and Bottrell *et al.* (1988): (1) favorable vein material was crushed to -10 to +40 mesh using a jaw crusher and iron mortar and pestle; (2) carbonates and clays were removed by boiling the samples in 1:1 standard reagent grade (SRG) HCl and HNO_3, rinsing with water, ultrasonically cleaning for at least 15 minutes, and rinsing again; (3) when necessary, samples were hand-picked; (4) the resulting material, mainly quartz, sometimes containing sulfides, was boiled in 1:1 SRG HCl and HNO_3 for four hours, washed in doubly distiled and deionized water (DDW), and boiled in DDW for one hour; (5) step four was repeated; (6) samples were put in electrolytic cleaning cells for a minimum of two weeks, changing the DDW periodically; (7) finally the samples were dried and put into clean containers until analysis.

Using approximately 10 g of sample material, fluid inclusion solutions were released by thermal decrepitation at 500°C in quartz glass decrepitation flasks. The fluid inclusion waters were collected by freezing them into capillary tubes for later hydrogen isotope analysis. The salts liberated by the decrepitation process were leached from the quartz using 30 to 50 ml of a 1 percent HNO_3, 200 ppm $LaCl_3$ solution. The quartz-solution mixture was allowed to sit at least a half hour before it was filtered using precleaned 0.2 μm nalgene filters. The leachate was reduced to dryness, rehydrated with 2 mls of 6 *N* HCl, and reduced to dryness again. The samples were stored in 5 ml teflon vials for transport to the University of New Mexico for final sample preparation and isotopic analysis as outlined in Ward, 1990.

Appendix B: Stable Isotope Analytical Methods

Hydrogen Isotopes

The waters analyzed for hydrogen isotopic values were liberated under vacuum by thermal decrepitation of quartz and calcite fluid inclusions at 500°C and collected by freezing into a glass capillary tube which was subsequently sealed with a glass blowing torch. At the time of isotopic analysis, the water was frozen into one end of the capillary tube, thawed, and then broken open. Three microliters of water were extracted from the open tube with another capillary tube.

Hydrogen isotopic analyses were performed by adding 3 microliters of sample water to 0.3 g of zinc reagent supplied by the Indiana University, Bloomington. The zinc reagent was prepared under vacuum by pumping on it in the reaction vessel for at least 30 minutes with periodically heating to remove any adsorbed water. Next, the reaction vessel was flooded with dry N_2 gas and a 3 µl capillary tube of sample was added. Then, the reaction vessel was sealed and the water frozen to the bottom. After the water was frozen, the reaction vessel was opened, the N_2 gas pumped away, and the reaction vessel resealed. At this point, the reaction vessel is removed from the vacuum line and placed in a heating block at 450°C for 30 minutes to convert the water into H_2 gas (modified from Coleman *et al.*, 1982). After the conversion of H_2O to H_2, the hydrogen isotope ratios are measured on the FinniganMAT Delta E stable isotope mass spectrometer.

The resulting data was corrected for a constant offset with respect to the values published for the National Bureau of Standards standards which were used to calibrate the process previously described. The equation used to correct the data is $y = 1.041x + 19.817$ in which x is the δD value measured by the mass spectrometer and y is the δD value corrected for the offset. The maximum variation observed for this technique for the samples analyzed was 9‰. Thus, at least two aliquots of sample water were analyzed whenever possible and the resulting isotopic values averaged. For samples FR-88-14, FR-88-29, and FR-88-30, only one analysis was obtained.

Due to concerns that the high temperatures of thermal decrepitation could fractionate the hydrogen isotopes, the techniques of thermal decreptitation and crushing which are used to liberate fluid inclusion waters were compared. The crushing procedure used 10 to 25 g of 0.2 to 1.0 cm pieces of sample material. The sample is crushed under vacuum in a stainless steel tube and liberated water is collected in a reaction vessel containing zinc reagent like the method above. At this stage, the two methods proceed identically and the sample is reacted and analyzed.

In this experiment, fluorite from the Hansonburg Mississippi Valley Type deposit in Bingham, NM, was used. Three runs of fluorite were prepared by crushing and two runs were prepared by thermal decrepitation. Two aliquots of water from each thermal decrepitation run were analyzed. The δD values ranged from -75 to -69‰ for the crushing runs and -74 to -69‰ for the thermally decrepitated runs. Essentially identical δD results from the two methods shows that the hydrogen isotopic composition of fluid inclusion waters liberated by thermal decrepitation are not fractionated significantly with respect to those liberated by crushing.

Oxygen Isotopes: Silicates

Oxygen gas was extracted from quartz for analysis using a ClF_3 reagent method (Borthwick and Harmon, 1982; Taylor and Epstein, 1962). Samples were crushed to a coarse powder and 10 to 15 mg of material were weighed out and placed into sample holders. The samples are oven dried at approximately 120°C for 2 hours. Then, the samples are loaded into nickle reaction vessels and reattached to a stainless steel vacuum line. After the pressure is reduced to approximately 0.08 torr, the samples are reacted with a 1.5 torr aliquot of ClF_3 reagent for 10 minutes at 150°C to remove any adsorbed water. The reaction vessels are evacuated of gas again and approximately 2.5 torr aliquot of reagent is added to react with the quartz for 8 hours at 450 to 500°C.

The resulting O_2 gas is converted to CO_2 gas by reaction with a heated carbon rod. This CO_2 gas is frozen into sample vessels for transport to the FinneganMAT Delta E stable isotope mass spectrometer in the lab where the oxygen isotope ratios are measured with respect to SMOW. Analyses of NBS-28 gave values averaging 9.72 ± 0.07‰.

The percent yield of O_2 gas from a sample was calculated from the weight of the sample reacted and the pressure of the resulting CO_2 gas. Some sample yields are over 100%. Since duplicate sample analyses have isotopic values within 0.3‰, the greater than 100% yields are believed to be the result of inaccurate calibration of the portion of the vacuum line used to measure the CO_2 gas pressure and not contamination by sample left over from previous use of the reaction vessels.

Carbon and Oxygen Isotopes: Carbonates

Calcite was reacted with 100% H_3PO_4 at 25°C for at least 8 hours to evolve CO_2 gas (McCrea, 1950). Carbon and oxygen isotopic ratios of the resulting CO_2 were measured with respect to PDB and SMOW respectively on the resulting CO_2 gas on a FinneganMAT Delta E stable isotope mass spectrometer. The oxygen isotope values were corrected for isotopic fractionation between the gas and the acid reagent. The corrections were determined by measuring the isotopic values of NBS-18, -19, and -20 and calculating the linear regression for the measured values and the actual values for the analyses that day.

Appendix C: Quantitative Gas Analysis Analytical Methods

Samples used for quantitative gas analysis were fractions of the same samples used for strontium analysis. One to 2.5 g of material was placed in a quartz glass decepitation flask and fixed to the vacuum line. The vacuum line was then pumped down to approximately 10^{-6} torr. During this time the sample was heated to 200°C for at least 2 hours to liberate any adsorbed water and surface nitrogen compounds that may have been left by the cleaning process. The gases were liberated by thermal decrepitation at 500°C and evaluated in three fractions: noncondensible gases, condensible gases, and water. The gases were analyzed using a Balzers quadrupole mass spectrometer at New Mexico Institute of Mining and Technology.

The concentration of gases were calculated by the standard inverted matrix method using the mass spectra and the probabilities of ionization. The noncondensible matrix considered the following gases: H_2, He, Ne, Ar, O_2, N_2, NO, NO_2, CO, CH_4, NH_3, HF, and H_2O. The condensible gas matrix considered these gases: CO_2, SO_2, H_2S, C_3H_6, C_4H_8, C_4H_{10}, C_5H_{10}, C_6H_6, CS_2, and H_2O.

TABLE C.1 Mass Spectra Sources

In house calibration	Balzers	Other
H_2	Ne	C_4H_8
He	Ar	C_5H_{10}
O_2	NO_2	
N_2	NH_3	
NO	HF	
CO	H_2O	
CH_4	C_3H_6	
CO_2	C_4H_8	
SO_2	C_4H_{10}	
H_2S	C_6H_6	
	CS_2	

The mass spectra of most gases were obtained either from in house calibration of the mass spectrometer used or from Balzers literature that accompanies the analytical software. Only two cracking outlines had to be obtained from another sources (Weast and Grasselli, 1990) (Table C.1).

The relative probability of ionization (RPI) factors, or sensitivities, as referred to N_2 gas with a value of 1.0 were either calculated from a known mixture of nitrogen and the gas in question, obtained from Balzers literature, or estimated by size and type of the molecule with respect to similar molecules in the Balzers literature (Table C.2). The sources of the RPI factors are listed in table C.2. The RPI factors for H_2, CH_4, and CO were first calculated for their gas and nitrogen mixture and then were adjusted to calculate the ratio of gases for a known mixture of H_2, CH_4, CO, and N_2.

TABLE C.2 Relative Probability of Ionization Values and Sources

In house calculation	Balzers	Estimates
H_2 (3.4)	Ne (0.3)	NO_2 (1.7)
CH_4 (2.0)	Ar (1.2)	C_3H_6 (3.7)
CO (0.8)	O_2 (1.0)	C_4H_8 (4.0)
He (1.3)	N_2 (1.0)	C_5H_{10} (5.5)
CO_2 (1.2)	NO (1.2)	
H_2S (1.2)	NH_3 (1.3)	
	HF (1.4)	
	SO_2 (2.1)	
	C_4H_{10} (4.9)	
	H_2O (1.0)	

The concentration of gases were corrected for excess H_2 gas created during the thermal decrepitation process using the unpublished computer program **GASFIX** by D.I. Norman. In addition, both gas fractions were analyzed for the presence of water in order to test the efficiency of the liquid N_2 trap and isopropal alcohol traps. Water contamination of the gas fractions was negligible, but when present the quantity of water was added to the total mole percent water.

Appendix D: Sample Stage, Depth, and Host Rock Information

Sample #	Stage	Depth (m)	Host rock
FR-88-6	II	270	Upr greywacke
FR-88-7	III	270	Chilitos andesite
FR-88-8	III	270	Chilitos andesite
FR-88-10	II	270	Chilitos andesite
FR-88-11	I	270	Chilitos andesite
FR-88-12	IV	270	Chilitos andesite
FR-88-13	II	270	Fresnillo Fmt
FR-88-14	II	270	Fresnillo Fmt
FR-88-15	I	270	Chilitos andesite
FR-88-16	I	270	Chilitos andesite
FR-88-19	I	295	Chilitos andesite
FR-88-20	II	295	Chilitos andesite
FR-88-21	III	295	Chilitos andesite
FR-88-24	I	320	Upr greywacke
FR-88-25	II	320	Upr greywacke
FR-88-28	III	320	Chilitos andesite
FR-88-29	III	320	Chilitos andesite
FR-88-30	I	320	Chilitos andesite
FR-88-31	II	320	Chilitos andesite
FR-88-32	II	370	Upr greywacke
FR-88-35	IV	350	Upr greywacke
FR-88-42	IV	370	Chilitos andesite
FR-88-43	I	370	Fresnillo Fmt
FR-88-47	II	425	Chilitos andesite
FR-88-50	III	425	Upr greywacke
FR-88-54	III	385	Upr greywacke
FR-88-55	IV	695	Upr greywacke
FR-88-56	I	695	Upr greywacke
FR-88-57	I	695	Upr greywacke
FR-88-58	I	695	Upr greywacke
FR-88-65	III	345	Chilitos andesite

This thesis is accepted on behalf of the faculty of the Institute by the following committee:

David L. Norton

Adviser

Andrew Campbell

William X. Clavez, Jr.

April 2, 1991

Date